

NGC 6712: the variable star population of a tidally disrupted globular cluster.[★]

D. Deras,^{1†} A. Arellano Ferro¹, C. Lázaro^{2,3}, I.H. Bustos Fierro⁴, J. H. Calderón^{4,5},
S. Muneer⁶, Sunetra Giridhar⁶

¹*Instituto de Astronomía, Universidad Nacional Autónoma de México, Ciudad Universitaria, C.P. 04510, México.*

²*Departamento de Astrofísica, Universidad de La Laguna, E-38206 La Laguna, Tenerife, Spain.*

³*Instituto de Astrofísica de Canarias (IAC), E-38205 La Laguna, Tenerife, Spain.*

⁴*Observatorio Astronómico, Universidad Nacional de Córdoba, Córdoba, Argentina.*

⁵*Consejo Nacional de Investigaciones Científicas y Técnicas (CONICET), Buenos Aires, Argentina.*

⁶*Indian Institute of Astrophysics, Koramangala 560034, Bangalore, India.*

Accepted XXX. Received YYY; in original form ZZZ

ABSTRACT

We present an analysis of VI CCD time series photometry of globular cluster NGC 6712. Our main goal is to study the variable star population as indicators of the cluster mean physical parameters. We employed the Fourier decomposition of RR Lyrae light curves to confirm that $[\text{Fe}/\text{H}]_{\text{UVES}} = -1.0 \pm 0.05$ is a solid estimate. We estimated the reddening to the cluster as $E(B - V) = 0.35 \pm 0.04$ from the RRab stars colour curves. The distance to the cluster was estimated using three independent methods which yielded a weighted mean distance $\langle d \rangle = 8.1 \pm 0.2$ kpc. The distribution of RRab and RRC stars on the HB shows a clear segregation around the first overtone red edge of the instability strip, which seems to be a common feature in OoI-type cluster with a very red horizontal branch. We carried out a membership analysis of 60,447 stars in our FoV using the data from *Gaia*-DR2 and found 1529 likely members; we possess the light curves of 1100 among the member stars. This allowed us to produce a clean colour-magnitude diagram, consistent with an age of 12 Gyrs, and enabled us to discover close unresolved contaminants for several variable stars. From the proper motion analysis we found evidence of non-member stars in the FoV of the cluster being tidally affected by the gravitational pull of the bulge of the Galaxy. We found that the RRab variable V6, shows a previously undetected Blazhko effect. Finally, we report sixteen new variables of the EW-type (9) and SR-type (7).

Key words: Globular clusters: individual: NGC 6712 – Stars: fundamental parameters – Stars: variables: RR Lyrae

1 INTRODUCTION

NGC 6712 is a small, sparse and metal rich globular cluster ($[\text{Fe}/\text{H}] = -1.02$; Harris (1996)) that can be found behind the Scutum stellar cloud ($\alpha = 18^{\text{h}}53^{\text{m}}04.32^{\text{s}}$, $\delta = -08^{\circ}42'21.5''$, J2000), and is located in the populated region of the Galactic bulge ($l = 25.35^{\circ}$, $b = -4.32^{\circ}$). Two versions of the Galactic orbit of the cluster can

be seen in Fig. 4. of Allen (1990) and in Fig. 18 of Ribeiro de Souza (2017). The orbit is asymmetrical, it is confined to within 2.0 kpc from the Galactic disc and penetrates deep into the Galactic center, reaching a galactocentric distance of 0.2-0.3 kpc (Dauphole et al. 1996; de Marchi et al. 1999). A recent estimation of the perigalacticon from *Gaia*-DR2 proper motions is 0.45 ± 0.10 kpc (Baumgardt et al. 2019). According to Cudworth (1988), the latest Galactic plane crossing could have happened as recently as ~4000 years ago, which is much smaller than its half-mass relaxation time of 1 Gyr (Harris 1996). Hence, repeated visits to the bulge and constant interaction with the disc in its 12 Gyrs, makes it very likely that this cluster has experienced several and strong tidal disruptions (Andreuzzi et al. 2001; Paltrinieri et al. 2001).

[★] Based on observations made with the telescope IAC80, in the Spanish Observatorio del Teide of the Instituto de Astrofísica de Canarias, in the island of Tenerife, Spain, and with the 2.0 m telescope at the Indian Astrophysical Observatory, Hanle, India.

[†] E-mail: dderas@astro.unam.mx, armando@astro.unam.mx, clh@iac.es, ivanbf@oac.unc.edu.ar, calderon@oac.unc.edu.ar, smuneer@iiap.res.in, giridhar@iiap.res.in

Theoretical calculations of the mass function lead to the suspicion that the $\sim 10^5 M_\odot$ (Pryor & Meylan 1993) cluster we see today is a remnant of the otherwise much more massive ($\sim 10^7 M_\odot$) cluster. This enormous mass loss may be reflected in the proper motions distribution, hence it is an added interest to explore the membership status of the stars in the field of the cluster and their motions in the light of the *Gaia*-DR2 data.

The variable star population of the cluster includes RR Lyrae, long-period semi-regular variables, short-period eclipsing binaries and an X-ray source whose counterpart presents optical variability (Pietrukowicz & Kaluzny 2004; Homer et al. 1996). The Catalogue of Variable Stars in Globular Clusters (CVSGC) (Clement et al. 2001), in its 2015 edition, lists 28 confirmed variables and summarises the history of their discovery between 1917 and 2004. The potential of variable stars to estimate mean metallicity, reddening and distance for the globular cluster is well known. High quality CCD photometry of the stars in the field of view of the cluster provide insights, not only on the pulsating properties of individual variables and potential discovery of new ones, but also enables the discussion of the Colour-Magnitude diagram (CMD) structure and its relation with the stellar evolution patterns and age of the system. In the present study we propose to undertake a *VI* CCD time-series analysis of NGC 6712.

The paper is structured as follows: In § 2 we detail the observations and reduction process of our images, § 3 we perform a membership analysis of the stars in our FoV to the cluster based on the *Gaia*-DR2 proper motions, in § 4 we describe our systematic search for variables and report new discoveries, in § 5 we describe the Fourier approach to estimate the physical parameters of the RR Lyrae stars, in § 6 we discuss the metallicity of the cluster employing alternative Fourier calibrations, in § 7 we present the cluster distance estimations by several independent methods, in § 8 we describe the structure of the CMD and the Horizontal Branch (HB), obtained from our photometry, in § 9 we briefly comment about the interaction of the cluster with the Galactic bulge and in § 10 we summarise our conclusions.

2 DATA, OBSERVATIONS AND REDUCTIONS

The data used in the present work were obtained from two sites. The first set of data was obtained with the 0.80 m IAC80 telescope at the Observatorio del Teide (Tenerife, Spain), during 10 non-consecutive nights, between June 13th and July 16th of 2016. We used the CAMELOT camera with 2048x2048 pixels and 0.304 arcsec/pixel, with a 10.4×10.4 arcmin² FoV, and a back illuminated detector CCD42-40 from E2V Technologies. The second set of data was obtained using the 2 m telescope at the Indian Astronomical Observatory (IAO) in Hanle, India on 12 nights separated into four intermittent seasons between June 2011 and April 2018. The detector used was a SITE ST-002 thinned backside illuminated CCD of 2048x2048 pixels with a scale of 0.296 arcsec/pix, translating to a field of view (FoV) of approximately 10.1×10.1 arcmin². The log of our observations is given in Table 1.

Table 1. The distribution of observations of NGC 6712 for each filter. Columns N_V and N_I give the number of images taken with the V and I filters respectively. Columns t_V and t_I provide the exposure time, or range of exposure times employed during each night for each filter. The average seeing is listed in the last column.

Date	N_V	t_V (s)	N_I	t_I (s)	Avg. seeing (")	site ¹
20110610	8	70-100	8	10	1.5	H
20110611	7	70-150	10	15-40	2.1	H
20110805	15	120-150	16	10-25	1.6	H
20110806	16	110-200	17	12-30	1.7	H
20130730	20	15-20	19	3-5	1.7	H
20150310	4	45	6	10	2.3	H
20150311	6	45	4	10	2.6	H
20150312	4	45	4	10	2.2	H
20150326	6	45	6	10	2.5	H
20150327	9	45-60	12	10-12	1.8	H
20160613	9	600-800	9	400-500	1.6	I
20160615	23	80-100	22	20-30	2.0	I
20160626	21	80-100	23	20-50	2.0	I
20160627	89	40-80	88	10-20	1.2	I
20160628	2	40-50	3	15	2.0	I
20160629	40	20	45	60	2.8	I
20160702	100	40-60	99	10-20	1.5	I
20160703	94	20-80	90	5-20	1.2	I
20160704	78	13-60	74	10-20	1.7	I
20160716	24	50-80	24	13-30	1.8	I
20180408	4	45	6	15	2.2	H
20180408	5	20	6	7	2.4	H
Total:	584	–	591	–	–	–

1. H: Hanle, I: IAC

2.1 Difference Image Analysis

The technique of Difference Imaging Analysis (DIA) with its pipeline implementation DanDIA¹ (Bramich 2008; Bramich et al. 2013) was used for the reduction of our data. This allowed us to obtain high-precision photometry for all the point sources in the FoV of the CCD. The software first creates a reference image by stacking the best images in each filter and then it subtracts them from the rest of the images in our collection. Using the PSF calculated by DanDIA from a sample of 300-400 isolated stars, we can determine the differential flux for each point source in the FoV. Then, the differential fluxes are converted into total fluxes. The total flux $f_{\text{tot}}(t)$ in ADU/s at each epoch t can be estimated as:

$$f_{\text{tot}}(t) = f_{\text{ref}} + \frac{f_{\text{diff}}(t)}{p(t)}, \quad (1)$$

where f_{ref} is the reference flux (ADU/s), $f_{\text{diff}}(t)$ is the differential flux (ADU/s) and $p(t)$ is the photometric scale factor (the integral of the kernel solution). Conversion to instrumental magnitudes was achieved using:

$$m_{\text{ins}}(t) = 25.0 - 2.5 \log [f_{\text{tot}}(t)], \quad (2)$$

where $m_{\text{ins}}(t)$ is the instrumental magnitude of the star at time t . A more detailed description of this method can be found in Bramich et al. (2011).

Systematic errors in our DIA photometry may be introduced

¹ DanDIA is built from the DanIDL library of IDL routines available at <http://www.danidl.co.uk>

due to a possible error in the flux-magnitude conversion factor (Bramich et al. 2015). To investigate their significance, we applied the methodology developed in Bramich & Freudling (2012) to solve for the magnitude offsets Z_k that should be applied to each photometric measurement from the image k . We found however, that in the present case the necessary corrections to our photometry were negligible (<0.001 mag).

2.2 Transformation to the standard system

In order to transform our light curves from the v instrumental magnitudes to the Johnson-Kron-Cousins standard V system, we made use of the standard stars in the field of NGC 6712 which are included in the online collection of Stetson (2000)². These stars are generally distributed in the cluster periphery. Unfortunately, this collection does not have the standard values for the I filter. Dr. Raúl Michel from the Observatorio Astronómico Nacional, México, made available to us his bulky observations of stars in the field of NGC 6712, that have been transformed into the I -standard system using the equatorial standards of Landolt (1983). We used 94 of these stars as standards to transform our IAC CCD photometry. For the Hanle set of data we identified 91 standard stars. The mild colour dependence of the standard minus instrumental magnitudes is shown in Fig. 1 for our observations. The transformation equations in both VI filters are explicitly given in the figure itself. We note that for the Hanle I -band transformation, the colour term is not significant and found that a linear transformation of the form $I = 1.024(\pm 0.006)i - 1.390(\pm 0.092)$ matches better the IAC and the Hanle I light curves.

3 STAR MEMBERSHIP USING GAIA

To determine cluster membership of the stars in our FoV, we used the high-quality astrometric data available in *Gaia*-DR2 (Gaia Collaboration et al. 2018). We employed the procedure developed by Bustos Fierro & Calderón (2019), consists of two stages: the first stage is based on the Balanced Iterative Reducing and Clustering using Hierarchies (BIRCH) algorithm (Zhang et al. 1996) in a four-dimensional space of physical parameters -gnomonic projection of celestial coordinates and proper motions- that detects groups of stars in this 4D space; in the second stage an analysis of the projected spatial distribution of stars with different proper motions allows the extraction of most of the members in the outskirts of the cluster or with large proper motions dispersion. Finally, it is checked that the extracted cluster members have their positions in celestial coordinates, the Vector Point Diagram (VPD) of the proper motions and the CMD (of Gaia photometric system) consistent with the characteristics of a globular cluster. We used a tidal radius of 8.5 arcmin from Harris (1996) (2010 edition) to set a boundary for the cluster and found 60 447 measured stars which we then cross-matched with our own data set. We found 1529 likely cluster members, for 1100 of which we possess light curves. In Fig. 2 we display the Vector Point Diagram (VPD) resulting from this membership analysis. The axes in the VPD correspond to the components of the proper motion vectors, therefore every proper motion is represented by a point. Since the cluster members share a common motion, they appear as a small concentration different

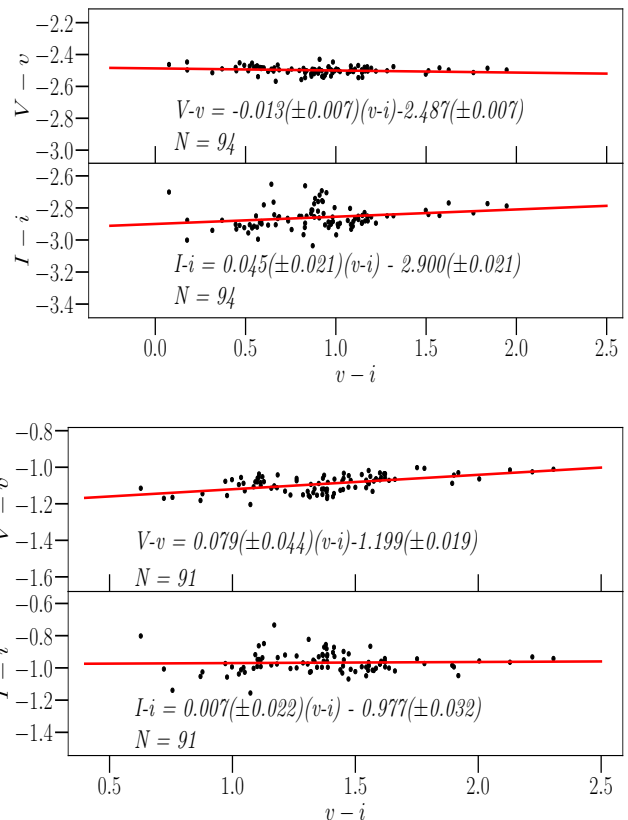


Figure 1. Transformation relations obtained for the V and I filters between the instrumental and the standard photometric systems. To carry out the transformation, we made use of a set of 94 and 91 standard stars for IAC (top panel) and Hanle (bottom panel) respectively, in the field of NGC 6712. The Hanle I -band color term is not significant, then a transformation of the form $I = 1.024(\pm 0.006)i - 1.354(\pm 0.093)$ was employed

from the wider distribution of field stars. Further comments on the cluster dynamics will be given later in § 9.

4 VARIABLE STARS IN NGC 6712

4.1 Search for new variables

In order to identify the variable star population in NGC 6712, we used several methods that we describe below. Our first approach was the use of the string-length method (Burke et al. 1970, Dworetzky 1983). We phased each light curve in our data with periods between 0.02 d and 1.7 d in steps of 10^{-6} d. In each case, the string-length parameter S_Q was calculated. The best phasing occurs when S_Q is minimum, and corresponds to the best period in our data. We then created a plot of the obtained minimum S_Q vs X-coordinate in our reference image for each light curve in our collection (Fig. 4). All variables in Table 3 and in Table 4 are identified. We note that most of the variables are located below an arbitrary threshold at 0.4, hence we individually explored each light curve below this value. Using this method, we identified two new cluster variables (V30 and V31) and seven new field variables (FV), FV1-FV7, all of which seem to be contact binaries or of the EW-type.

The second method was to explore the regions of the CMD where variable stars are expected to be found. In particular, we explored the stars near the tip of the Red Giant Branch (TRGB) and

² <http://www3.cadc-ccda.hia-ihp.nrc-cnrc.gc.ca/community/STETSON/standards>

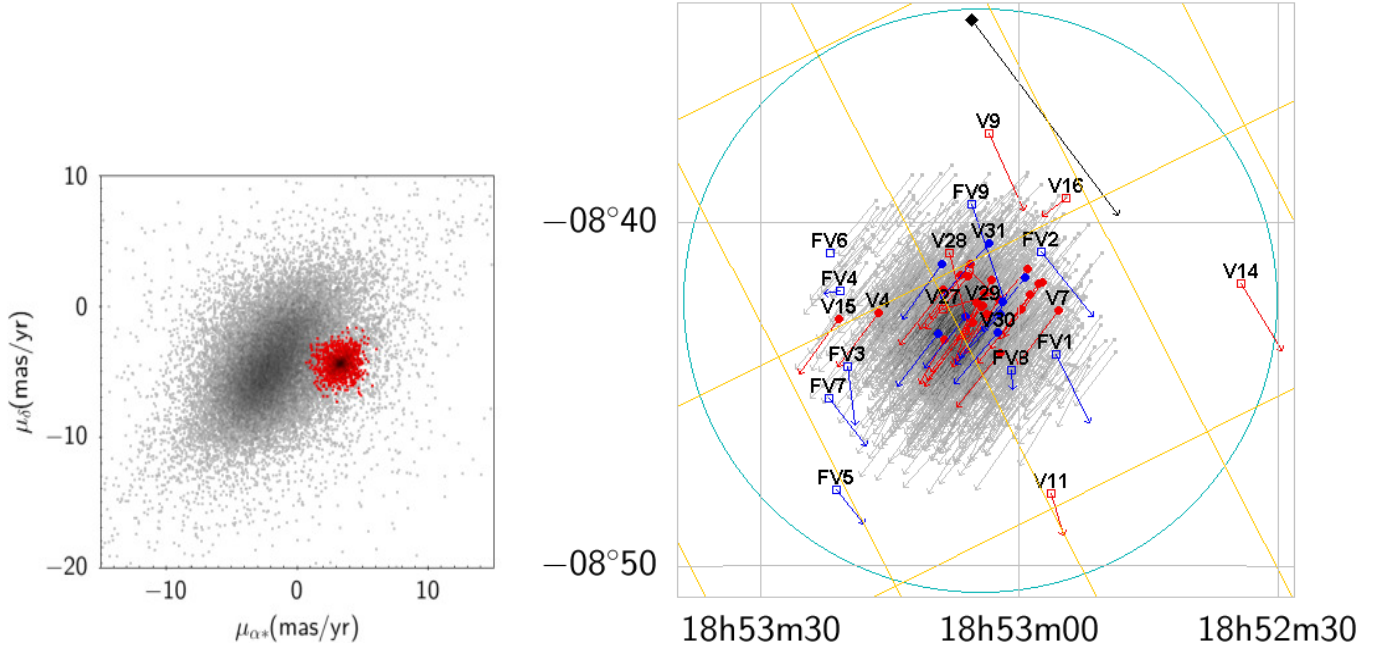


Figure 2. Left panel: Vector Point Diagram of the stars within a $8.5'$ radius. Grey dots are field stars and red dots are cluster members. Right panel: Projection on the sky of the proper motion vectors. Grey arrows are used for member stars, red arrows for known cluster variables, blue arrows for new variable stars reported in this work, red open circles for known field variables and blue open circles for new field variables. The yellow grid corresponds to the Galactic l and b coordinates. The large black arrow indicates the direction of the Galactic center. Vectors have been enlarged 20000x for visualisation purposes. See § 9 for further discussion.

Table 2. Time-series VI photometry for the variables stars observed in this work*

Variable Star ID	Filter	HJD (d)	M_{std} (mag)	m_{ins} (mag)	σ_m (mag)
V1	V	2455723.42031	16.611	17.723	0.006
V1	V	2455723.42540	16.601	17.714	0.007
...
V1	I	2455723.41738	15.622	16.608	0.008
V1	I	2455723.42325	15.631	16.617	0.012
...
V2	V	2457555.59991	12.610	15.120	0.001
V	V	2457555.60211	12.611	15.121	0.001
...
V2	I	2457555.60101	10.564	13.386	0.001
V2	I	2457555.60322	10.553	13.375	0.001
...

* The standard and instrumental magnitudes are listed in columns 4 and 5, respectively, corresponding to the variable stars in column 1. Filter and epoch of mid-exposure are listed in columns 2 and 3, respectively. The uncertainty on m_{ins} is listed in column 6, which also corresponds to the uncertainty on M_{std} . A full version of this table is available at the CDS database.

we found 4 new semi-regular or SR variables (V32-V35), a SR-type field variable (FV8) and a SR candidate (which we will denote as C) for which we are unsure of its variation.

The last method used was to plot the rms vs. mean magnitude of all the stars in our FoV (Fig. 5). We performed the search in regions where variable stars such as RR Lyrae and SR type stars are usually located. With this approach we identified two more SR-type variable stars (V36, and FV9).

In Fig. 3 we present an identification chart with all known and

newly found variables at present, including those that may not be cluster members. It is important to mention that in our data set we were not able to recover the light curves of V9 and V14 since they are out of our FoV, V11 since it lies near the lower border of our reference image and was not measured, and V25 since it is below the limit of our photometry. Notice that V25 is an X-ray source (LXMB), with a faint optical counterpart. We also found that several of the known variable stars are non-cluster members, namely, V9, V11, V14, V16, V17, V27, V28 and V29, according to the method used to determine stellar membership described in § 3. The time-series VI photometry obtained in this work is reported in Table 2, of which only a small portion is included in the printed version of the paper. The full table shall be available in electronic form in the Centre de Données astronomiques de Strasbourg database (CDS).

4.2 RR Lyrae stars in NGC 6712

In the 2015 edition of the CVSGC, there are listed 8 RRab, 6 RRC and one RR Lyrae without mode classification. The present data and a careful inspection of the resulting light curves, made necessary it to reclassify some stars, namely V22, V23 and V27, as RRab, RRab and EW, respectively. The details of these new classifications are explained in Appendix A. As a result, the RR Lyrae population of NGC 6712 is formed by 10 RRab and 4 RRC stars. Our observations generally cover the light curves phase reasonably well, with the exception of V12, the reason being its nearly half-day periodicity that operates against a better phase coverage. In order to confirm its light curve shape and pulsation mode type, we complemented our V data with V data of Sandage et al. (1966). While the scatter of these observations is large, they confirm the RRab-type nature of this star. In spite of this, V12 shall not be considered for

Table 3. Data of member variable stars in NGC 6712 in the FoV of our images.

Star ID	Type	$\langle V \rangle$ (mag)	$\langle I \rangle$ (mag)	A_V (mag)	A_I (mag)	P (days)	HJD _{max} + 2450000	α (J2000.0)	δ (J2000.0)	Gaia-DR2 Source
V1	RRab	16.31	15.40	1.11	0.75	0.512039	7574.6054	18:52:59.85	-08:42:31.3	4203848946351463808
V2	SR	12.55	10.50	>0.15	>0.07	109.0 ¹	—	18:53:08.79	-08:41:56.8	4203849393028208384
V3	RRab	16.24	15.26	0.57	0.38	0.655956	7574.6678	18:53:02.29	-08:43:47.4	4203848877631995136
V4	RRab	16.47	15.41	0.56	0.36	0.611745	7574.6268	18:53:16.29	-08:42:38.1	4203849122517862144
V5	RRab	16.41	15.44	1.14	0.74	0.545362	7572.6357	18:53:08.68	-08:43:24.1	4203848778920519168
V6	RRab <i>Bl</i>	16.45	15.56	0.86	0.59	0.510871	7553.6906	18:53:05.35	-08:42:53.6	4203848985005261312
V7	M	16.98 ⁷	11.97 ⁷	>0.62	>0.23	193.0 ²	—	18:52:55.39	-08:42:32.6	4203849672273972864
V8	SR	13.17 ⁷	10.90 ⁷	>0.48	>0.28	116.29 ²	—	18:53:05.66	-08:41:12.4	4203849461747677056
V10	L	13.94 ⁷	11.27 ⁷	>0.21	—	—	—	18:52:57.35	-08:41:43.9	4203849874064515456
V12	RRab	16.30	—	1.21	—	0.502790	5284.7907	18:53:06.02	-08:41:33.4	4203849088158338944
V13	RRab	16.13	15.26	1.02	0.66	0.562655	7574.6637	18:52:57.77	-08:41:46.5	4203849809712937088
V15	L	13.83 ⁷	11.08 ⁷	>1.5	—	—	—	18:53:20.99	-08:42:48.2	4203837401469330944
V18	RRc	16.15	15.32	0.47	0.28	0.353543	7569.5876	18:53:02.44	-08:42:14.0	4203849053798612096
V19	RRc	16.00	15.19	0.40	0.24	0.412161	7586.6633	18:53:03.22	-08:41:39.2	4203849844072610816
V20	RRc	16.20	15.48	0.34	0.25	0.250521	5779.3246	18:53:04.16	-08:42:03.7	4203849083790434304
V21	L	13.58 ⁷	11.26 ⁷	>0.33	—	—	—	18:52:58.80	-08:42:06.2	4203849805344920576
V22	RRab ³	16.17	15.24	0.58	0.41	0.654789	7586.6187	18:52:59.08	-08:41:20.5	4203849874064518016
V23	RRab ⁴	16.23	15.26	0.31	0.19	0.642451	7572.6241	18:53:03.83	-08:42:39.4	4203848985005549056
V24	RRab	16.23	15.25	0.99	0.61	0.576454	7586.6334	18:53:04.37	-08:42:26.9	4203849053725057280
V26	RRc	16.16	15.64	0.12	0.09	0.334317	7569.6551	18:53:06.80	-08:41:31.2	4203849466042002944
V28	EW	18.23	17.42	0.26	0.08	0.434497	7573.6734 ⁷	18:53:08.09	-08:40:52.2	4203849466042155264
V29	EW	18.45	16.95	—	—	0.453571	7569.6226 ⁷	18:53:04.17	-08:42:25.0	4203849053798521472
V30 ⁵	EW	18.68	17.91	0.61	0.49	0.504748	7567.6482 ⁷	18:53:02.51	-08:43:11.9	4203848881926249600
V31 ⁵	EW	18.53	17.74	0.40	0.38	0.418762	7573.6734 ⁷	18:53:03.49	-08:40:34.4	4203850221956827648
V32 ⁵	SRs	13.72 ⁶	11.56 ⁶	>0.14	>0.06	31.1	7586.6252	18:52:59.32	-08:41:34.7	4203849805345042176
V33 ⁵	SR	13.68 ⁶	11.57 ⁶	>0.24	—	—	—	18:53:06.20	-08:42:43.2	420384985079013760
V34 ⁵	SR	13.54 ⁶	11.59 ⁶	>0.25	—	—	—	18:53:01.99	-08:42:18.8	4203849049430686336
V35 ⁵	SR	13.93 ⁶	12.00 ⁶	>0.17	—	—	—	18:53:09.02	-08:41:12.4	4203849461747685760
V36 ⁵	SRs	13.66 ⁶	11.79 ⁶	>0.22	>0.11	17.8	5724.4243	18:53:09.39	-08:43:12.9	4203848808912547840
C ⁸	SRs	13.84 ⁶	11.64 ⁶	>0.21	—	18.9	5780.3438	18:53:02.30	-08:42:38.4	4203849049430685312

1. The period is from Oosterhoff (1943). 2. The period is from Sloan et al. (2010). 3. Classified as RRab in this work. See § A3. 4. Reclassified as RRab in this work. See § A4. 5. New variable discovered in this work. 6. Magnitude-weighted mean. 7. Time of primary minimum light. 8. Member variable candidate. *Bl* denotes Blazhko effect.

Table 4. Data of known, unclassified and newly discovered field variable stars (FV) in NGC 6712 in the FoV of our images.

Star ID	Type	$\langle V \rangle$ (mag)	$\langle I \rangle$ (mag)	A_V (mag)	A_I (mag)	P (days)	HJD _{min} + 2450000	α (J2000.0)	δ (J2000.0)	Gaia-DR2 Source
V16	?	14.98 ⁷	14.16 ⁷	>0.06	>0.06	—	—	18:52:54.55	-08:39:17.0	4203850187670201088
V17	?	14.89 ⁷	14.23 ⁷	>0.24	—	—	—	18:53:05.86	-08:41:23.4	4203849083790555520
V27	EW ¹	16.51	15.34	0.12	0.08	0.425714	7586.6325 ²	18:53:08.88	-08:42:30.7	4203849019364947456
FV1 ⁴	EW	18.25	17.14	0.54	0.48	0.354499	7574.6363 ²	18:52:55.78	-08:43:49.1	4203847438817518976
FV2 ⁴	EW	17.84	16.65	0.27	0.25	0.355390	7567.5873 ²	18:52:57.45	-08:40:50.4	4203849874064515840
FV3 ⁴	EW	14.44	13.66	0.38	0.35	0.445495	7574.6047 ²	18:53:19.90	-08:44:10.1	4203837298410747776
FV4 ⁴	EW	17.04	16.07	0.23	0.19	0.368598	7572.6428 ²	18:53:20.86	-08:41:58.9	4203849259956801792
FV5 ⁴	EW	18.93	17.96	0.54	0.54	0.347863	7572.6380 ²	18:53:21.25	-08:47:46.5	4203835756498276608
FV6 ⁴	EW	18.39	17.41	0.40	0.39	0.462812	7573.8535 ²	18:53:21.90	-08:40:52.2	4203849362961930624
FV7 ⁴	EW	17.88	16.74	0.72	0.51	0.344416	7567.6514 ²	18:53:22.04	-08:45:06.3	4203836718651092352
FV8 ⁴	SRs	14.17 ³	10.74 ³	>0.58	—	12.3	7555.6001	18:53:00.93	-08:44:18.1	4203848843272252160
FV9 ⁴	SRs	13.45 ³	10.17 ³	>0.15	—	24.6	8217.4473	18:53:05.58	-08:39:27.6	4203850325109041792

1. Reclassified as EW in this work. See § A6. 2. Time of primary minimum light. 3. Magnitude-weighted mean. 4. New variable discovered in this work.

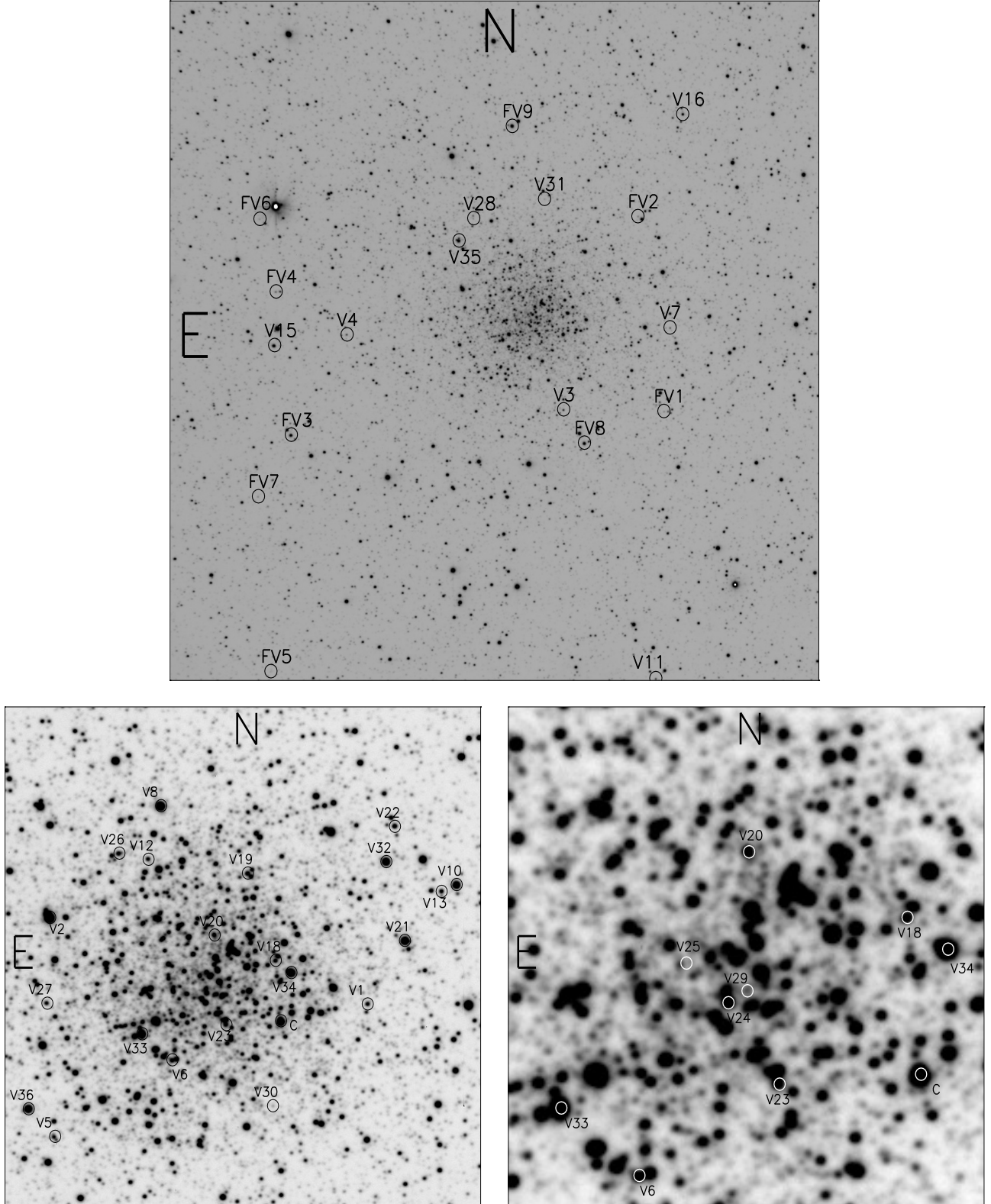


Figure 3. Identification chart for all known and newly discovered variables in NGC 6712. The bottom two diagrams show the central regions of the cluster and some stars are identified in more than one panel: The field sizes of the three panels are 10.4×10.4 , 3.3×3.3 and 1.3×1.3 arcmin², respectively. Variables labelled 'FV' are field stars according to our proper motion analysis (see § 3). The marker V25 shows no star but this is an X-ray source (LMXB) (Homer et al. 1996) not visible in our images.

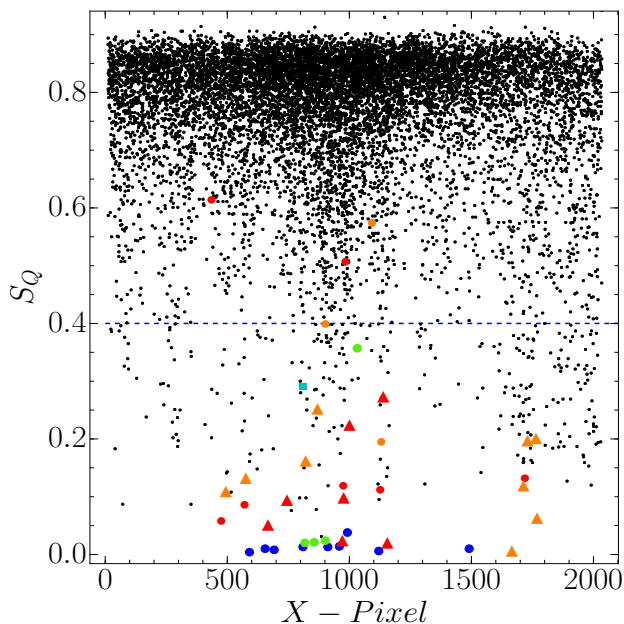


Figure 4. Minimum value for the string-length parameter S_Q calculated for the 11,294 stars with a light curve in our V reference image, versus CCD X-pixel coordinate. The blue circles correspond to a RRab stars, green circles to RRc stars, red circles and triangles correspond to semi-regular variables and orange circles and triangles to EW stars. The cyan square denotes a SR-variable candidate. Triangles are used for the newly discovered variables. The dashed blue line is an arbitrary threshold set at 0.4, below which most of the known variables are located. See § 4.1 for a discussion.

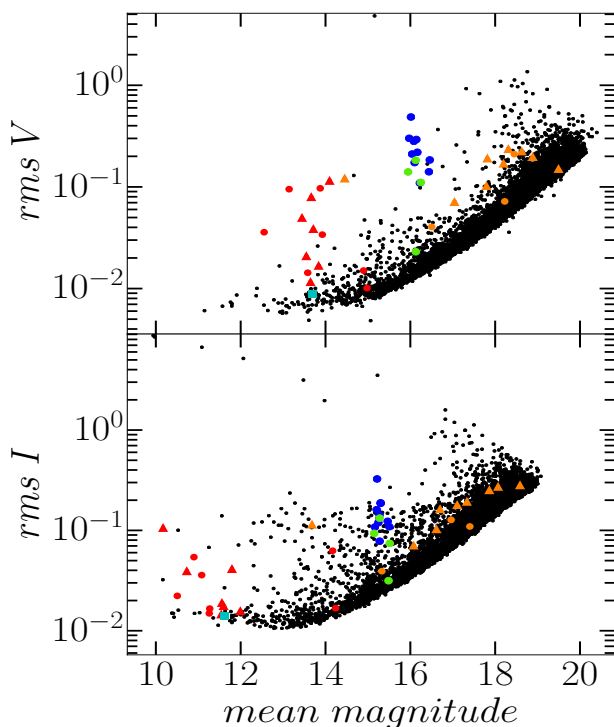


Figure 5. The rms magnitude deviations as a function of the mean magnitudes V and I . The blue circles correspond to a RRab stars, green circles to RRc stars, red circles correspond to semi-regular variables and orange circles and triangles to EW stars. The cyan square denotes a SR-variable candidate. Triangles are used for the newly discovered variables.

the physical parameters calculations. With the inclusion of the data from Hanle, we were also able to detect a mild modulation in the amplitude of the light curve of V6. This suggests the presence of a previously undetected Blazhko effect. The light curves of all RR Lyrae are shown in Fig. 6.

4.2.1 Bailey diagram and Oosterhoff type

The period-amplitude plane for RR Lyrae stars, also known as the Bailey diagram, is a useful tool as it clearly segregates pulsation modes, helps defining the Oosterhoff type of a given cluster, and identifies RRab stars that may be advanced in their evolution towards the asymptotic giant branch (AGB). The diagram for NGC 6712 is shown in Fig. 7 for the VI band passes. The periods and amplitudes are listed in Table 3. The amplitudes were measured from the corresponding fit provided by the Fourier decomposition of their light curves (See § 5). The average of the periods of the RRab stars in NGC 6712 is $\langle P_{ab} \rangle = 0.58 \pm 0.02$, which classifies it as a OoI-type cluster. The RRab and RRc stars in this diagram occupy the loci that has been observed to be consistent with the definition of a OoI-type globular cluster (black solid lines in V and I filters, respectively). V6 is classified as a RRab-type star, nevertheless, it is located at an odd position on the Bailey diagram, which can be explained due to its Blazhko nature. We note that V5 is located along the evolved star sequence, however, its position of the CMD lies very close to the ZAHB and without a formal analysis of a possible secular period change, we cannot state its evolutionary status relative to the rest of the RR Lyrae stars.

4.3 Semi-regular variable stars in NGC 6712

There are seven known semi-regular or long-period variables, classified as SR or L in the CVSGC, namely, V2, V7, V8, V10, V14, V15 and V21. Unfortunately V14 lies outside our FoV and was not measured. Without a sufficiently long time-base and dense data set, the classification of long-term semi-regular variables is always dubious. Our Hanle and IAC data sets span eight years, which enables to peer the long-term light behaviour. On the other hand, the more continuous pace of the observations at the IAC, enabled us to analyse even the short-term behaviour. Additionally, we found seven semi-regular variables and have tagged them as SR-type stars. Five of these stars are cluster members (V32-V36) and two are not (FV8 and FV9). In Fig. 8 the light curves of the above stars are displayed. The insets in the figure show the short-term light curve behaviour and sometimes suggest a periodicity. A proper period search in all these light curves allowed us to find reliable periods in five of these stars, listed in Tables 3 and 4. The corresponding phased light curves are displayed in Fig. A1

4.4 Eclipsing binaries in the field of NGC 6712

The catalogue of Clement et al. (2001) lists two W Ursae Majoris-type binaries or EW stars (V28 and V29), first reported by Pietrukowicz & Kaluzny (2004). We were able to recover their light curves from our data and to identify nine new eclipsing binaries present in our FoV. The V and I light curves are shown in Fig. 9. The light curves present a morphology typical of the W UMa contact systems, except V30 which presents a steeper descent to minimum and is probably not a contact binary. V27 was previously misidentified as a RRc star (see § A6).

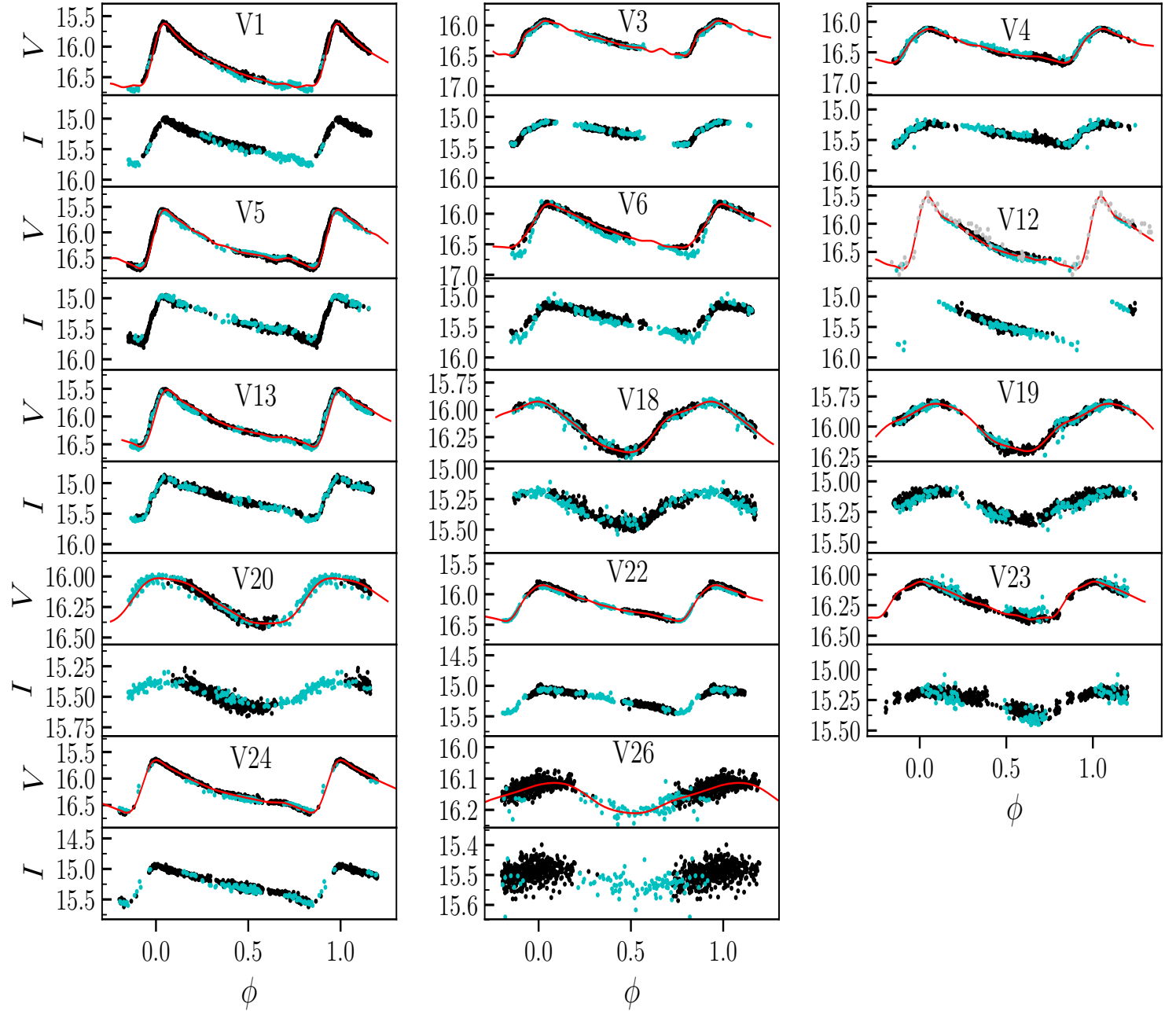


Figure 6. RR Lyrae stars in NGC 6712. Black and cyan symbols correspond to observations from IAC and Hanle respectively. The red line represents the Fourier fit. Note that the scale in the Y-axis is different for RRab and RRC stars. The grey dots in V12 come from [Sandage et al. \(1966\)](#) and were used to complete our light curve in the V-band. (See § 5).

From the study of cluster membership using *Gaia*-DR2, most of the new binaries seem to be field stars, and so their reddening and distances are unknown. In order to get some information from their photometric light curves we have assumed they are contact systems. Based on *Gaia*-DR1, [Chen et al. \(2018\)](#) de-

rived period-luminosity relations for W UMa-type systems, of the form $M_{\lambda}(\max)_C = a_{\lambda} \log P + b_{\lambda}$, claiming 8% distance accuracy, where P is the orbital period. We have used the 3D

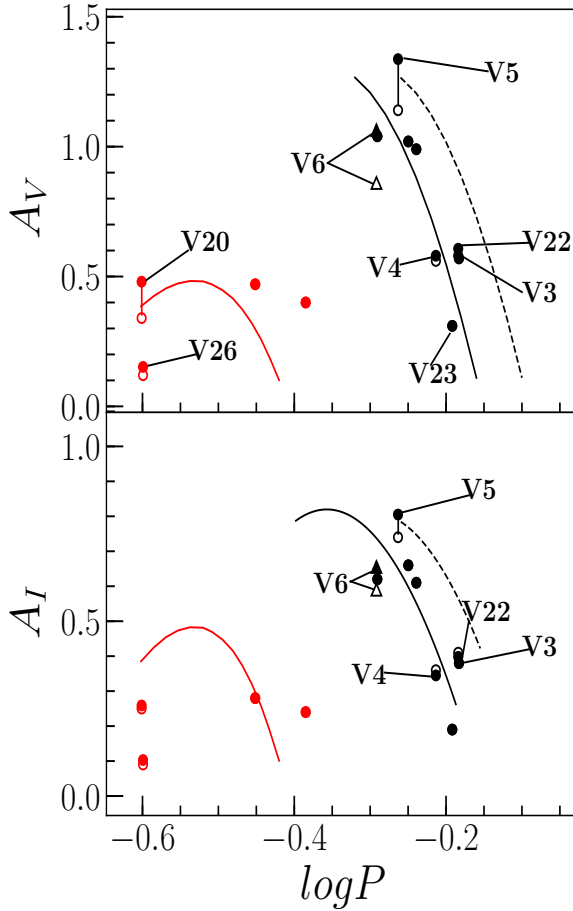


Figure 7. Bailey diagram for NGC 6712. Filled black and red symbols represent RRab and RRc stars respectively. The open symbols denote the original position of the RR Lyrae before a correction to their amplitude was performed due to contamination of a neighbour star. The triangular marker (V6) is a Blazhko RRab star. The continuous and dashed black lines in the top panel are the loci for unevolved and evolved stars according to Cacciari et al. (2005). The red parabolas were calculated by Arellano Ferro et al. (2015) from RRc stars in five OoI clusters. In the bottom panel, the black solid and segmented loci for unevolved and evolved stars respectively are from Kunder et al. (2013). See § 4.2.1 for a more detailed discussion.

Dust Mapping ³ facility to get the increase of $E(B - V)$ with distance, looking for the best agreement between $M_{\lambda}(max)_C$ and $M_{\lambda} = m_{\lambda}(max) - A_{\lambda} - 5 \log d(pc) + 5$, for each one of the systems in the VI bands. The $E(B - V)$ in the direction of the cluster changes from ~ 0.13 at 2 kpc, to ~ 0.37 - 0.40 at 7.9 kpc. The results are given in the columns 2 and 3 of Table 5, and are consistent with the *Gaia*-DR2 membership study, supporting the hypothesis that most of them are closer than the cluster.

With a value for $E(B - V)$, we can derive the intrinsic colours $(V - I)_o$ of the binaries, used to estimate the effective temperatures of the components from the calibration $(V - I)_o - T_{\text{eff}}$ of Huang et al. (2015), and the relative contribution of each component to the total flux in V and I, calculated in the light curves fits. The VI light curves have been modelled with the code BinaRoche (Lázaro et al. 2009), weighting in the fits the deviations of both components from the mass-radius relations of Awadalla & Hanna (2005) for W UMa

binaries. The derived parameters of the fits are given in Table 5, while the observed and model light curves are shown in Fig. 9. The collected data of V30 cover only one of the eclipses, which has been arbitrarily considered to be the primary, with a steeper descent than other light curves, and could be a detached or semidetached binary.

Given the assumptions implicit in the analysis, and the quality of the light curves, we prefer not to put an error bar in the tabulated values. A realistic estimation of the uncertainties can be about ± 300 K in the $T_{\text{eff},1}$ effective temperatures, affected by the $E(B - V)$ used to deredden the observed $(V - I)$ colour. The ratios $T_{2/1} = T_{\text{eff},2}/T_{\text{eff},1}$ and $q = M_2/M_1$ are determined by the photometric quality of the light curves, and its uncertainty can be about ± 0.02 . The most uncertain parameter is the primary mass M_1 , but with these values the models put the systems at distances similar to those given in column 3.

5 RR LYRAE STARS: [FE/H] AND M_V FROM LIGHT CURVE FOURIER DECOMPOSITION

The light curves of RR Lyrae stars exhibit periodic oscillations and are hence well represented by a Fourier series of the following form:

$$m(t) = A_0 + \sum_{k=1}^N A_k \cos\left(\frac{2\pi}{P} k(t - E_0) + \phi_k\right) \quad (3)$$

where $m(t)$ is the magnitude at time t , P is the period of pulsation, and E_0 is the epoch. To estimate the Fourier parameters we followed a least-squares approach, where the quantities to be minimised are the amplitudes A_k and phases ϕ_k of the light curve components. The Fourier parameters, i.e., the amplitudes and phases of the harmonics in Eq. 3 are defined as $R_{ij} = A_i/A_j$ and $\phi_{ij} = j\phi_i - i\phi_j$, respectively. The estimated Fourier coefficients for the RR Lyrae stars in our data are listed in Table 6.

We have employed the calibrations of Jurcsik & Kovács (1996) (JK96) and Kovács & Walker (2001) to calculate the metallicity and absolute magnitude of the RRab stars. The specific set of equations used in this work is listed below.

$$[\text{Fe}/\text{H}]_J = -5.038 - 5.394 P + 1.345 \phi_{31}^{(s)}, \quad (4)$$

$$M_V = -1.876 \log P - 1.158 A_1 + 0.821 A_3 + K. \quad (5)$$

These calibrations have an associated uncertainty of 0.14 dex and 0.04mag for the metallicity and the absolute magnitude respectively. Since the metallicity is given in the Jurcsik-Kovács scale, we can transform it to the standard Zinn-West scale (Zinn & West 1984) with the following equation: $[\text{Fe}/\text{H}]_J = 1.431[\text{Fe}/\text{H}]_{ZW} + 0.88$ (Jurcsik 1995). For eq. 5, we adopted the zero point $K = 0.41$ from the analysis of Arellano Ferro et al. (2010).

For the RRc stars, we adopted the calibrations given by Morgan et al. (2007) and Kovács & Kanbur (1998), respectively:

$$[\text{Fe}/\text{H}]_{ZW} = 52.466 P^2 - 30.075 P + 0.131 \phi_{31}^{2(c)} - 0.982 \phi_{31}^{(c)} - 4.198 \phi_{31}^{(c)} P + 2.424, \quad (6)$$

³ <http://argonaut.skymaps.info>

Table 5. Physical Parameters of EW stars in NGC 6712 in the FoV of our images (§ 4.4). Stars labelled FV are not cluster members.

Star ID	$E(B - V)$	d (kpc.)	$M_1(M_\odot)$	q	$T_{\text{eff},1}$ (K)	$T_{2/1}$	R_1 (R_\odot)	R_2 (R_\odot)	$i(^{\circ})$
V27	0.21	2.8	1.37	0.93	5530	0.94	1.26	1.12	39.6
V28	0.36	6.3	1.30	0.40	7480	0.98	1.33	0.83	45.0
V30	0.37	7.9	0.48	0.60	9750	0.60	0.88	0.74	77.5
V31	0.37	6.3	0.45	1.0	9700	0.72	0.86	0.86	68.3
FV1	0.35	4.0	0.92	0.99	6200	0.99	1.00	1.00	74.8
FV2	0.29	4.0	1.19	0.44	5840	0.92	1.16	0.80	63.6
FV3	0.15	1.2	1.24	0.98	6220	0.98	1.26	1.25	68.0
FV4	0.19	3.2	0.95	0.87	5850	0.98	1.01	0.96	56.1
FV5	0.41	7.0	0.77	0.99	7110	0.98	0.90	0.91	80.0
FV6	0.36	6.3	1.40	0.85	7300	0.75	1.29	1.13	83.4
FV7	0.21	3.2	0.80	1.0	5800	0.90	0.92	0.92	79.0

$$M_V = 1.061 - 0.961 P - 0.044 \phi_{21}^{(s)} - 4.447 A_4. \quad (7)$$

These calibrations have an associated uncertainty of 0.14 dex and 0.042mag for the metallicity and the absolute magnitude respectively. One can transform the coefficients from cosine series phases into sine series using the following relation, if needed:

$$\phi_{jk}^{(s)} = \phi_{jk}^{(c)} - (j - k) \frac{\pi}{2}. \quad (8)$$

The Fourier coefficients of the RR Lyrae stars identified in NGC 6712 are listed in Table 6, and in Table 7 we report the physical parameters derived from the Fourier decomposition. In their paper, JK96 propose a test that validates the usability of the Fourier coefficients obtained from the Fourier decomposition of the light curves of RRab stars. They suggest that the values of the iron abundance [Fe/H] obtained are only valid if their *Deviation Parameter* or *Dm* does not exceeds the value of 3.0. The *Dm* value for each RRab star is listed in Table 6 in column 10.

The iron abundance in the scale of Zinn & West (1984) can be converted into the high-dispersion spectroscopy (HDS) or UVES scale of Carretta et al. (2009) via the equation $[\text{Fe}/\text{H}]_{\text{UVES}} = -0.413 + 0.130[\text{Fe}/\text{H}]_{\text{ZW}} - 0.356[\text{Fe}/\text{H}]_{\text{ZW}}^2$, and are also listed in Table 7.

The values of M_V reported in Table 7 have been transformed to luminosities using the following equation:

$$\log(L/L_\odot) = -0.4(M_V - M_{\text{bol}}^\odot + \text{BC}). \quad (9)$$

To calculate the bolometric correction, we used the equation $\text{BC} = 0.06[\text{Fe}/\text{H}]_{\text{ZW}} + 0.06$ as derived by Sandage & Cacciari (1990). We have adopted the value of $M_{\text{bol}}^\odot = 4.75$ mag.

The effective temperature of the RRab stars was estimated with the calibration given by Jurcsik (1998):

$$\log(T_{\text{eff}}) = 3.9291 - 0.1112(V - K)_0 - 0.0032[\text{Fe}/\text{H}], \quad (10)$$

where

$$(V - K)_0 = 1.585 + 1.257P - 0.273A_1 - 0.234\phi_{31}^{(s)} + 0.062\phi_{41}^{(s)}. \quad (11)$$

For the effective temperature in RRC stars, we used:

$$\log(T_{\text{eff}}) = 3.7746 - 0.1452\log(P) + 0.0056\phi_{31}^{(c)}, \quad (12)$$

as derived by Simon & Clement (1993). We can also estimate the masses of the RR Lyrae stars using: $\log(M/M_\odot) =$

$16.907 - 1.47\log(P_F) + 1.24\log(L/L_\odot) - 5.12\log(T_{\text{eff}})$ as given by van Albada & Baker (1971) where P_F is the fundamental period. The stellar mean radii can be obtained from $L = 4\pi R^2 \sigma T^4$. These values are also reported in Table 7.

6 FURTHER COMMENTS ON THE METALLICITY OF NGC 6712

NGC 6712 is a moderately metal-poor OoI-type cluster from which Harris (1996) reports a metallicity of $[\text{Fe}/\text{H}] = -1.02$. For our estimation of the metallicity, we did not use the RRab stars V4, V6 and V23 since the value of their *Dm* parameter is larger than 3.0. For V6, its light curve also shows a mild Blazhko-like amplitude modulation which affects the value of its physical parameters. In the case of V12, we recall that its light curve is incomplete due to its period being nearly half-day and although its *Dm* value is smaller than 3.0, the uncertainties in its physical parameters are very large, and therefore was not taken into account for the averages. Following the Fourier decomposition method described in § 5, we found an average $[\text{Fe}/\text{H}]_{\text{UVES}}^{\text{JK96}} = -1.13 \pm 0.02$ given in HDS scale (Carretta et al. 2009).

It has been recognised that the calibration of JK96 produces metallicities too rich by ~ 0.3 dex for extremely metal poor stars (e.g. JK96, Smolec (2005)). For more metal-rich stars the differences between spectroscopic values and those from the JK96 calibration are small (Smolec 2005). The present results offer a good opportunity to test the prediction of JK96 calibration for the high metallicity extreme, being NGC 6712 among the most metal-rich globular clusters. Nemec et al. (2013) (N13) proposed new formulations to derive photometric values on the HDS scale for the RRab and RRC stars, using non-linear model between HDS values of [Fe/H] and the Fourier parameter ϕ_{31} , in a broader metallicity range, particularly at the lower end of [Fe/H]. For completeness we reproduce here their formulations.

For the RRab stars,

$$[\text{Fe}/\text{H}] = b_0 + b_1 P + b_2 \phi_{31}^{(s)}(Kp) + b_3 \phi_{31}^{(s)}(Kp) P + b_4 (\phi_{31}^{(s)}(Kp))^2, \quad (13)$$

with the coefficient values $b_0 = -8.65 \pm 4.64$, $b_1 = -40.12 \pm 5.18$, $b_2 = 5.96 \pm 1.72$, $b_3 = 6.27 \pm 0.96$ and $b_4 = -0.72 \pm 0.17$, and a rms error of 0.084 dex. The Fourier parameter $\phi_{31}^{(s)}(Kp)$, is calculated from the light curve in the Kepler photometric system,

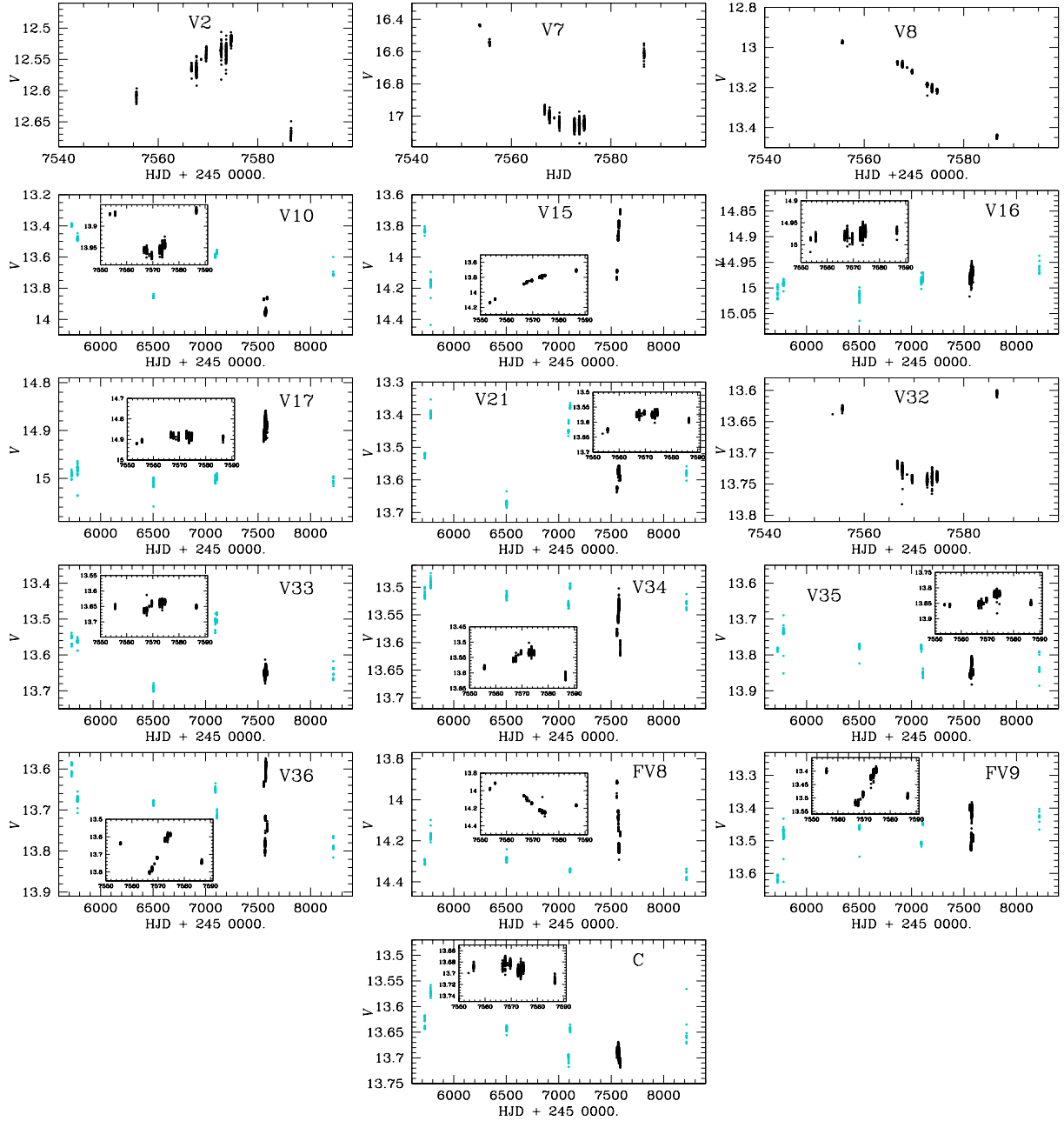


Figure 8. SR stars in NGC 6712. Colour symbols are as in Fig. 6. The full time-span is of nine years and the long-term variation is evident. The insets display a blow up of the IAC data (black symbols) for which a smoother and continuous pace is available, and the variation in a shorter time span is shown. Stars with no inset lack Hanle data due to saturation. See § 4.3.

thus, our Fourier parameters from the V light curve listed in Table 6 were transformed into the Kepler system via the relation: $\phi_{31}^{(s)}(Kp) = \phi_{31}^{(s)} + 0.151$ (Nemec et al. 2011) before applying the calibration.

For the RRc stars,

$$[\text{Fe}/\text{H}] = b_0 + b_1 P + b_2 \phi_{31}^{(c)} + b_3 \phi_{31}^{(c)} P + b_4 P + b_5 (\phi_{31}^{(c)})^2, \quad (14)$$

with the coefficient values $b_0 = 1.70 \pm 0.82$, $b_1 = -15.67 \pm 5.38$, $b_2 = 0.20 \pm 0.21$, $b_3 = -2.41 \pm 0.62$, $b_4 = 18 \pm 8.70$, and $b_5 = 0.17 \pm 0.04$, and a rms error of 0.13 dex. The Fourier parameter $\phi_{31}^{(c)}$ is straight that given in Table 6.

We used these formulations to calculate the individual values

$[\text{Fe}/\text{H}]_{\text{UVES}}^{\text{N13}}$ listed in column 4 of Table 7 and the weighted averages -0.82 ± 0.06 for the RRAb stars and -0.96 ± 0.19 for the RRc stars. The weighted average of these two values is -0.85 ± 0.05 , which is in good agreement with the value reported by Ferraro et al. (1999a) of $[\text{Fe}/\text{H}]_{\text{UVES}}^{\text{N13}} = -0.88$. These values of the iron-to-hydrogen ratio, in the HDS scale, should be compared to the values of $[\text{Fe}/\text{H}]_{\text{UVES}}^{\text{JK96}}$ given in column 3 of Table 7, i.e. the transformation of the values in the ZW scale, into the HDS or UVES scale established by Carretta et al. (2009). In conclusion, the N13 calibrations give slightly higher iron-to-hydrogen abundances for this metal poor cluster than the JK96 calibration, however, the difference is small and both determinations agree reasonably well with

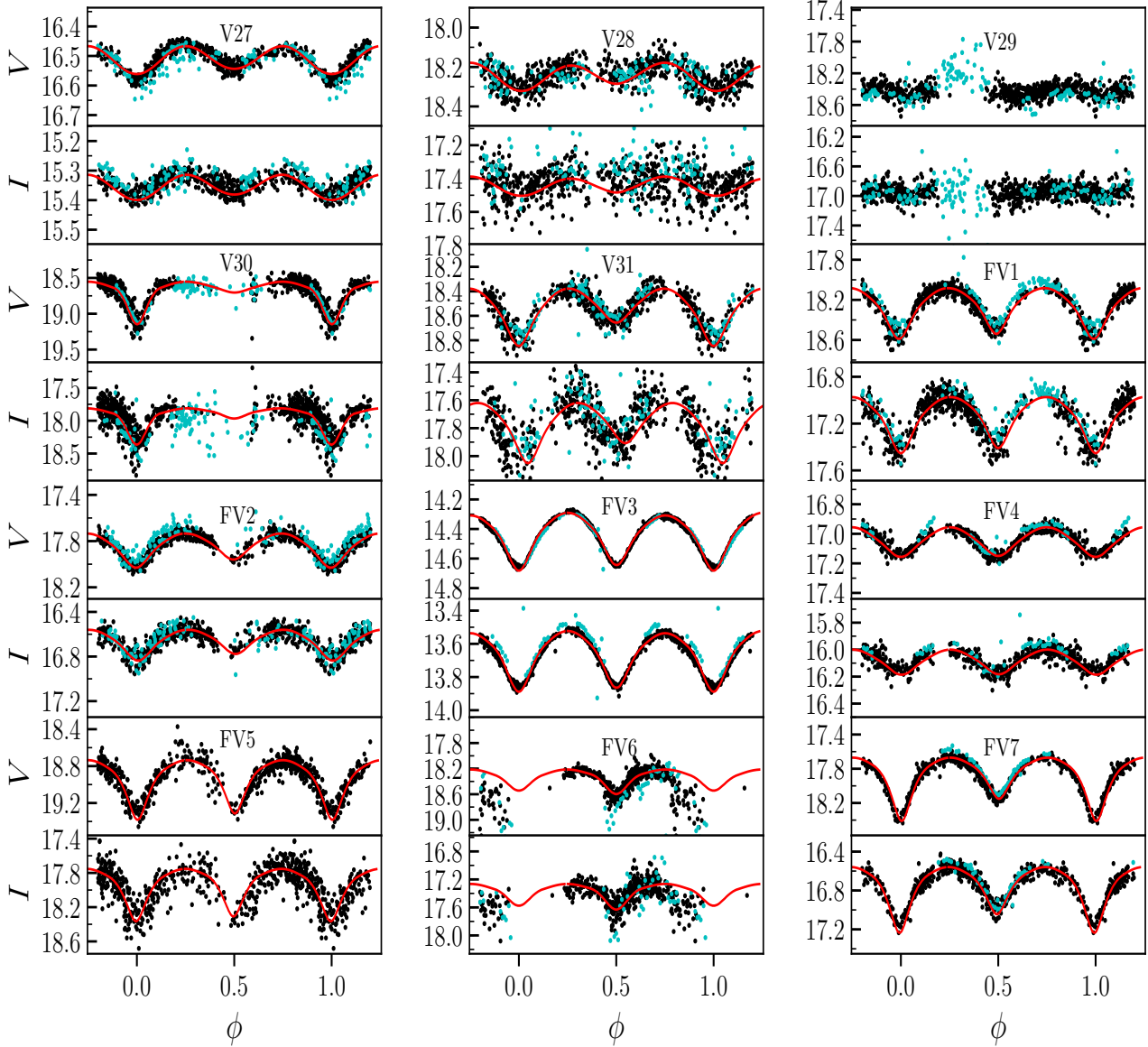


Figure 9. EW stars in NGC 6712. Black and cyan symbols correspond to observations from IAC and Hanle respectively. Red continuous curves are the model solution. The stars V30, V31 and FV1-FV7 are newly discovered variables. See § 4.4.

the value of -1.0 dex adopted in the compilation of [Harris \(1996\)](#). Later we shall return to the metallicity issue when we compare isochrones for a given metallicity with the observed star distribution in the CMD (See § 8).

7 ON THE DISTANCE TO NGC 6712

7.1 The reddening of NGC 6712

The determination of an accurate value for the interstellar reddening is fundamental in the estimation of a distance to NGC 6712.

In his catalogue, [Harris \(1996\)](#) (2010 edition) reports a reddening of $E(B - V) = 0.45$ although there is no consensus in the literature with respect its actual value. In order to obtain an independent estimate for the reddening, we followed the method used by [Sturch \(1966\)](#), according to which, RRab stars have a constant intrinsic colour $(B - V)_0$ near minimum light, between phases 0.5 and 0.8. We also made use of the calibration of $(V - I)_0$ in this range of phases derived by [Guldenschuh et al. \(2005\)](#) as $(V - I)_{0,min} = 0.58 \pm 0.02$ mag. This allowed us to estimate the individual values of $E(V - I)$ for six RRab stars, namely, V4, V5, V13, V22, V23 and V24. We then converted to $E(B - V)$ using the ratio

Table 6. Fourier coefficients A_k for $k = 0, 1, 2, 3, 4$, and phases from the cosine series $\phi_{21}^{(c)}$, $\phi_{31}^{(c)}$ and $\phi_{41}^{(c)}$, for RRab and RRc stars. The numbers in parentheses indicate the uncertainty on the last decimal place. Also listed is the deviation parameter D_m for the RRab stars (see JK96).

Star ID	A_0 (V mag)	A_1 (V mag)	A_2 (V mag)	A_3 (V mag)	A_4 (V mag)	$\phi_{21}^{(c)}$	$\phi_{31}^{(c)}$	$\phi_{41}^{(c)}$	D_m
RRab stars									
V1	16.311(2)	0.381(3)	0.182(3)	0.111(3)	0.071(3)	4.120(25)	8.286(37)	6.185(55)	1.4
V3	16.238(12)	0.221(2)	0.092(2)	0.050(2)	0.022(3)	4.305(36)	8.790(57)	7.336(114)	2.1
V4	16.428(1)	0.209(2)	0.097(2)	0.056(2)	0.018(2)	4.211(27)	8.660(49)	7.197(126)	5.7
V5	16.253(2)	0.379(3)	0.202(3)	0.128(3)	0.093(2)	4.037(20)	8.349(30)	6.482(58)	2.5
V6	16.257(2)	0.292(2)	0.118(2)	0.052(3)	0.020(2)	4.251(27)	8.740(53)	6.711(134)	6.3
V12	16.343(3)	0.422(4)	0.219(4)	0.142(4)	0.104(5)	3.999(30)	8.369(45)	6.351(60)	1.7
V13	16.133(1)	0.345(2)	0.182(2)	0.114(1)	0.076(1)	4.086(12)	8.438(18)	6.608(28)	1.3
V22	16.166(1)	0.226(1)	0.102(1)	0.051(1)	0.022(1)	4.315(18)	8.931(31)	7.344(66)	2.3
V23	16.225(1)	0.140(1)	0.041(1)	0.013(1)	0.008(1)	4.442(38)	9.013(119)	7.755(233)	8.9
V24	16.228(2)	0.329(2)	0.180(2)	0.111(2)	0.071(1)	4.156(18)	8.564(29)	6.821(37)	1.2
RRc stars									
V18	16.151(1)	0.226(2)	0.012(2)	0.019(2)	0.012(2)	5.775(132)	4.629(92)	2.901(140)	-
V19	16.000(1)	0.192(2)	0.014(2)	0.012(2)	0.012(2)	7.1176(125)	4.836(145)	4.159(135)	-
V20	16.202(3)	0.190(3)	0.011(3)	0.008(3)	0.006(3)	3.156(322)	2.119(475)	6.918(465)	-
V26	16.162(1)	0.047(2)	0.007(2)	0.018(2)	0.015(1)	7.7262(260)	4.7131(1024)	4.989(1000)	-

Table 7. Physical parameters obtained from the Fourier fit for the RRab and RRc stars. The numbers in parentheses indicate the uncertainty on the last decimal place. See § 5 for a detailed discussion.

RRab stars								
Star ID	[Fe/H] _{ZW} ^{JK96}	[Fe/H] _{UVES} ^{JK96}	[Fe/H] _{UVES} ^{N13}	M_V	$\log T_{\text{eff}}$	$\log(L/L_{\odot})$	M/M_{\odot}	R/R_{\odot}
V1	-1.23(4)	-1.11(3)	-0.82(6)	0.605(4)	3.819(9)	1.658(2)	0.68(7)	5.20(1)
V3	-1.30(5)	-1.18(5)	-0.77(10)	0.539(3)	3.800(20)	1.685(1)	0.65(11)	5.87(1)
V4 ¹	-1.26(5)	-1.14(4)	-0.80(8)	0.614(3)	3.803(20)	1.654(1)	0.63(12)	5.59(1)
V5	-1.30(3)	-1.18(3)	-0.94(5)	0.570(4)	3.815(9)	1.672(2)	0.69(8)	5.41(1)
V6 ¹	-0.80(5)	-0.74(3)	-0.26(5)	0.662(3)	3.823(20)	1.635(1)	0.62(12)	4.98(1)
V12 ¹	-1.12(42)	-1.00(34)	-0.64(6)	0.598(6)	3.822(10)	1.661(2)	0.68(8)	5.15(1)
V13	-1.28(2)	-1.16(2)	-0.90(3)	0.574(2)	3.812(8)	1.670(1)	0.67(6)	5.45(1)
V22	-1.16(4)	-1.05(4)	-0.53(5)	0.535(1)	3.803(10)	1.686(1)	0.63(7)	5.79(1)
V23 ¹	-1.04(11)	-0.93(8)	-0.39(16)	0.619(1)	3.801(27)	1.652(1)	0.60(19)	5.63(1)
V24	-1.21(3)	-1.09(2)	-0.78(4)	0.569(3)	3.812(8)	1.672(1)	0.66(6)	5.48(1)
Weighted Mean	-1.25	-1.13	-0.82	0.551	3.812	1.679	0.66	5.64
σ	± 0.02	± 0.02	± 0.06	± 0.039	± 0.003	± 0.001	± 0.01	± 0.08
RRc stars								
V18	-1.17(23)	-1.05(19)	-0.97(10)	0.476(11)	3.866(1)	1.710(4)	0.51(1)	4.45(2)
V19	-1.64(45)	-1.58(52)	-1.60(16)	0.355(10)	3.857(1)	1.758(4)	0.52(1)	4.90(2)
V20	-0.96(19)	-0.87(13)	-0.87(7)	0.650(5)	3.878(1)	1.640(2)	0.61(1)	3.90(1)
Weighted Mean	-1.10	-0.95	-0.96	0.572	3.869	1.671	0.56	4.09
σ	± 0.16	± 0.17	± 0.19	± 0.070	± 0.005	± 0.028	± 0.03	± 0.24

1. Not included in the [Fe/H] averages.

$E(V - I)/E(B - V) = 1.259$ derived by Schlegel et al. (1998). This yielded a mean reddening $E(B - V) = 0.35 \pm 0.04$ which we have adopted for our calculations. The light curves were phased with the periods listed in Table 3 and the values for the reddening of each star used are in Table 8. Evidences of differential reddening in the region of NGC 6712 were offered by Janulis & Smriglio (1992), which can explain the inconsistencies found in the literature for the several reddening estimations, which will impact the determination

of the distance to the cluster. See for instance table 3 in Janulis & Smriglio (1992) and a further discussion in § 7.4.

7.2 From the RR Lyrae stars

From the Fourier decomposition of the light curves of the RRab and RRc stars and the empirical calibrations for the absolute magnitude M_V given in § 5, we found a distance of 8.1 ± 0.3 kpc and a distance

Table 8. Reddening estimations from RRab stars.

Star ID	$E(B - V)$
V4	0.409 ± 0.005
V5	0.330 ± 0.015
V13	0.308 ± 0.007
V22	0.335 ± 0.003
V23	0.326 ± 0.023
V24	0.388 ± 0.008
Mean	0.349
σ	± 0.036

of 8.0 ± 0.3 kpc, respectively. As an independent estimation for the distance, we also made use of the P-L relation for RR Lyrae stars in the *I*-band (Catelan et al. 2004), $M_I = 0.471 - 1.132 \log P + 0.205 \log Z$, with $\log Z = [M/H] - 1.765$; $[M/H] = [\text{Fe}/H] - \log(0.638 f + 0.362)$ and $\log f = [\alpha/\text{Fe}]$, from where we adopted $[\alpha/\text{Fe}] = +0.3$ (Salaris et al. 1993). With the aforementioned relation, we derived a distance of 8.3 ± 0.3 kpc. The value of the extinction coefficient adopted was $A_V = 3.1E(B - V)$. We used all the RR Lyrae stars listed in table 6.

7.3 Luminous Red Giants as distance indicators

A method that was originally developed to determine distances to nearby galaxies (Lee et al. 1993) can in principle be used to determine the distance to a globular cluster, using the luminosity of the brightest stars near the tip of the red giant branch (TRGB). The bolometric magnitude of the TRGB can be estimated from the cluster metallicity via the equation (Salaris & Cassisi 1997):

$$M_{bol}^{tip} = -3.949 - 0.178 [M/H] + 0.008 [M/H]^2, \quad (15)$$

where $[M/H] = [\text{Fe}/H] - \log(0.638 f + 0.362)$ and $\log f = [\alpha/\text{Fe}]$ (Salaris et al. 1993).

When using this method, one should be aware of two things: first, this method strongly depends on an adequate selection of the stars used, and second, that the brightest stars in a given cluster may not actually be at the tip of the RGB in the CMD, but rather beneath it by a certain magnitude. Viaux et al. (2013) argued that, in low-mass stars, the neutrino magnetic dipole moment, may delay the helium ignition and result in the extension of the red giant branch, and that, in the case of M5 the brightest stars are between 0.04 and 0.16 mag below the TRGB. The suggested offset was confirmed by the non-canonical models of Arceo-Díaz et al. (2015); from the analysis of 25 globular clusters these authors concluded that the theoretical TRGB is in average about 0.26 ± 0.24 bolometric magnitudes brighter than the one observed. Using eq. 15 and the SR-type star members in the cluster, we estimated its distance and found that if we use a correction of 0.1 mag, V8 and V15, which are near the TRGB following the course of the two extreme isochrones in Fig. 10, yield values of 8.0 kpc and 8.2 kpc respectively, which are in good agreement with the estimated distances obtained by the other methods discussed previously. This probably suggests that the true TRGB in NGC 6712 is located at about 0.1 mag above these stars.

7.4 Cluster distance inconsistencies

The RR Lyrae star light curve Fourier decomposition and the *I*-band P-L relationship lead to a distance of about 8.1 ± 0.2 kpc (Ta-

Table 9. Distance comparison to NGC 6712 from the different methods used in this work.

Method	Distance [kpc]
RRab Fourier decomposition	8.1 ± 0.3
RRc Fourier decomposition	8.0 ± 0.3
RRab / RRc <i>I</i> -band P-L	8.3 ± 0.3

ble 9) if a reddening $E(B - V) = 0.35$ is assumed (§ 7.1 and Table 8). This value is over one kiloparsec larger than 6.9 kpc for $E(B - V) = 0.45$ adopted by Harris (1996), and the kinematic value 6.95 ± 0.39 kpc obtained by Baumgardt et al. (2019) from the analysis of *Gaia*-DR2 proper motions and radial velocities. We must stress that if $E(B - V) = 0.45$ is adopted, our Fourier and P-L values would result in a distance of 7.0 ± 0.2 kpc. The galactic dust maps and calibrations of Schlegel et al. (1998) and Schlafly & Finkbeiner (2011) give $E(B - V)$ values of 0.397 ± 0.007 and 0.342 ± 0.006 respectively. The 3D Dust Mapping facility mentioned in 4.4 suggests the increase trend of $E(B - V)$ with distance in a given direction, and suggests for NGC 6712, $E(B - V) \sim 0.37$ -0.40 at 7.9 kpc. Thus we consider very unlikely that the reddening is above 0.40, in which case the distance yielded by our methods is hardly below 7.5 ± 0.2 kpc. However, we must add that, if a reddening of 0.40 is taken, the isochrones and ZAHB of the CMD will appear unacceptably shifted to the red (see § 8). Thus, the RR Lyrae distance and our approaches lead to a distance, given the respective uncertainties, marginally larger than the kinematic result. Finally, we want to point out to two independent photometric reddening and distance determinations for NGC 6712: $E(B - V) = 0.33$ and 7.9 ± 1.0 kpc (Ortolani et al. 2000) and $E(B - V) = 0.33 \pm 0.05$ and ~ 8.0 kpc (Paltrinieri et al. 2001). Both values were obtained by considering that the colour of the RGB at the level of the HB of the globular cluster NGC 6712 is a close analogue to NGC 6171. This difference in colour yields $\Delta(B - V)_{\text{NGC6712-NGC6171}} = 0.0$, meaning that these two have the same reddening.

8 THE COLOUR-MAGNITUDE DIAGRAM OF NGC 6712

Given its position near the Galactic Bulge, NGC 6712 presents a highly contaminated CMD. This can be seen in Fig. 10, left panel. From their *BV* photometry and constraining to stars within a radius $r < 47''$, Ortolani et al. (2000) managed to clean the CMD, but no membership analysis was actually carried out.

With the method described in § 3, we were able to remove the field stars and obtained a remarkably clean CMD, see Fig. 10, right panel. This allowed us to overlay three isochrones, one with a metallicity of $[\text{Fe}/H] = -1.25$ (blue), which comes from the value obtained from the Fourier decomposition of the light curves of the RR Lyrae stars, another with the metallicity of $[\text{Fe}/H] = -1.0$ (red) reported by Harris (1996) and one with $[\text{Fe}/H] = -0.86$ (green) derived from the equations of N13, given in § 6. The three isochrones were shifted to a distance of 8.1 kpc and have been reddened by $E(B - V) = 0.35$. The isochrones were calculated from the models of VandenBerg et al. (2014) with $Y = 0.25$ and $[\alpha/\text{Fe}] = +0.4$, and they correspond to an age of 12 Gyrs. It is evident that the two isochrones with extreme metallicities, bracket the one for $[\text{Fe}/H] = -1.0$, which, despite the scatter at the RGB, particularly near the tip, seems to produce the best fit. In other words, the observed CMD supports the conclusion that $[\text{Fe}/H] = -1.0$ is indeed a

solid estimation. The iron-to-hydrogen calibrations of JK96 and of N13, discussed in sections 5 and 6 respectively, agree, within their own uncertainties, with this value of the metallicity.

Like the isochrones, a ZAHB of metallicity $[\text{Fe}/\text{H}]=-1.31$ (VandenBerg et al. 2014) was placed in the CMD. No significant differences were observed for other metallicities. The resulting position of the ZAHB is consistent with the distance of 8.1 kpc.

8.1 The structure of the Horizontal Branch of NGC 6712

Once the CMD has been cleaned from field stars using the method described in § 3, it displays a prominent red HB and a sparsely populated blue tail which is typical of OoI-type clusters. The RR Lyrae population on the HB is dominated by fundamental mode RRab pulsators (10) in comparison with first overtone pulsators (4). The distribution of RRab and RRc shows a clear mode segregation around the First Overtone Red Edge (FORE) if one accepts that the FORE may be shifted to the blue by a few hundredths of a magnitude, of the otherwise established position (see Fig. 10), which given the uncertainties, it is quite likely. We can also see that V22 (RR Lyrae with no previous classification) and V23 (originally classified as RRc) clearly fall on the right side of the FORE of the IS which along with their period, light curve shape, and position in the Period-Amplitude diagram (Fig. 4.2.1) confirm their nature as RRab stars.

While plotting all the positions of the *Gaia* sources in our FoV, we noticed that two sources, not resolved in our photometry, fall within the FWHM of the PSF of some of the RR Lyrae stars, namely V4, V5, V6, V20, V22 and V26. The data of the two *Gaia* sources for each variable are listed in Table 10. Hence, their magnitude and colour are contaminated by the extra flux of the neighbour. A correction to their positions on the HB was performed by measuring the combined flux in the G , G_{BP} , and G_{RP} -band, of both sources, and converting them to the Johnson V_{GAIA} and I_{GAIA} magnitudes. For this purpose we used the relations provided by J.M. Carrasco (2018: *Gaia* team), available in Section 5.3.7 of the *Gaia*-DR2 documentation⁴. The magnitudes of the two sources were combined to calculate V_{mix} and I_{mix} , and the corrections $\Delta V = V_{GAIA} - V_{mix}$ and $\Delta I = I_{GAIA} - I_{mix}$ where then added to the intensity-weighted means $\langle V \rangle$ and $\langle I \rangle$ (Table 3) calculated from our light curves, i.e., to estimate their apparent magnitude without the flux contamination of the neighbouring star. This also helped us to recalculate the amplitude for these stars and, in doing so, their position in the Bailey diagram 4.2.1. In the lower panel of Fig. 10 we plot the corrected positions of the aforementioned RR Lyrae stars.

At this stage, we can comment on the RR Lyrae pulsating-mode distribution and their relation with the HB overall structure. A parameter that is useful in describing the morphology of the HB is the Lee parameter (Lee 1990) defined as $\mathcal{L} = (B - R)/(B + V + R)$ where B , V and R are the number of stars to the blue, inside and to the red of the IS. For NGC 6712, we estimated from the clean CMD of Fig. 10, $\mathcal{L} = -0.44$. For the sake of comparison, Paltrinieri et al. (2001) reported $\mathcal{L} = -0.66$, although they estimated this value by constraining the stars in their FoV to a radius $<5'$ so it might still include some foreground stars on the HB which would make up for the difference with respect to our estimated value. It has been highlighted in several recent studies, e.g. Arellano Ferro et al. (2019) (their figure 8), that the RRab and RRc stars may be cleanly

separated by the FORE or that a mixture of modes can be found in the bi-modal region, also sometimes referred to as the either-or region. And, that this condition seems to be correlated with the overall structure parameter \mathcal{L} and the Oosterhoff type. There are six OoI-type clusters with very red HB's ($\mathcal{L} < -0.5$), Rup 106, NGC 362, NGC 1261, NGC 6171, NGC 6362 and NGC 6712; for NGC 362 there is no detailed study of the mode distribution and Rup 106 has no known RRc stars. In the bottom panel of Fig. 10 we note that V13 might be the only RRab star sitting in the bimodal region. However, given the uncertainties in the stellar colours and the positioning of the FORE the two modes could be considered as being segregated, in which case, in NGC 6712, like in the other three, NGC 1261, NGC 6171 and NGC 6362, the modes are well separated. This property is also observed in all OoII-type clusters thus far studied but only in some OoI-type clusters of intermediate values for \mathcal{L} .

8.2 Comments on the blue-straggler population of NGC 6712

Paltrinieri et al. (2001), based on their $V - (B - V)$ CMD, identified 108 candidate blue-straggler stars (BSS) in the central region of NGC 6712. The cluster being a very compact object, finding a large number of BSS does not come as a surprise, since they may originate in stellar collisions (Ferraro et al. 1999b). The BSS region in our CMD does not look so much populated. We identified 61 cluster members in this region after cleaning for the non-members through the proper motion analysis (§ 3). We also found two contact binaries among these BSS, V30 and V31. Thus, we are inclined to believe that NGC 6712 does not have a large population of BSS as previously suggested by Paltrinieri et al. (2001)

9 COMMENTS ON THE NGC 6712 CLUSTER TIDAL IDENTITY

As we have briefly summarised in the introduction, there are numerous evidences that favour the idea that NGC 6712 was once was a very massive globular cluster in the Galaxy, and that after numerous close encounters with the Galactic bulge, and the constant interaction with the disc, it has been tidally stripped of nearly 99% of its mass (Andreuzzi et al. 2001; Paltrinieri et al. 2001). To what extent do these tidal disrupting forces imprint their evidence in the remaining cluster core? The unprecedented accurate proper motions in the *Gaia*-DR2 are the best observations available at present to investigate this question. The proper motion vectors, projected on the plane of the sky, of the 1529 cluster member stars identified in § 3 are shown in the bottom panel of Fig. 2, where it is evident that the whole cluster moves as a compact entity, and the stars in solidarity maintain their identity. This is contrary to what is seen for instance in Pal 13 (Yepez et al. 2019) (their figure 12), a rather loose cluster being tidally disrupted.

However, we note in the bottom panel of Fig. 2, that some apparent field variables (labelled in the figure) have proper motions that are consistently nearly perpendicular to the cluster motion, parallel to the Galactic longitude and towards the Galactic centre. This suggests that these stars participate in the local Galactic rotation, as expected in field stars, and not in the present orbital motion of the cluster.

It is also fair to say that based solely on the proper motions of the stars in our FoV, we are unable to tell the difference between the ones belonging to the field and the ones that are actually being or starting to be stripped away from the cluster.

⁴ <http://gea.esac.esa.int/archive/documentation/GDR2/index.html>

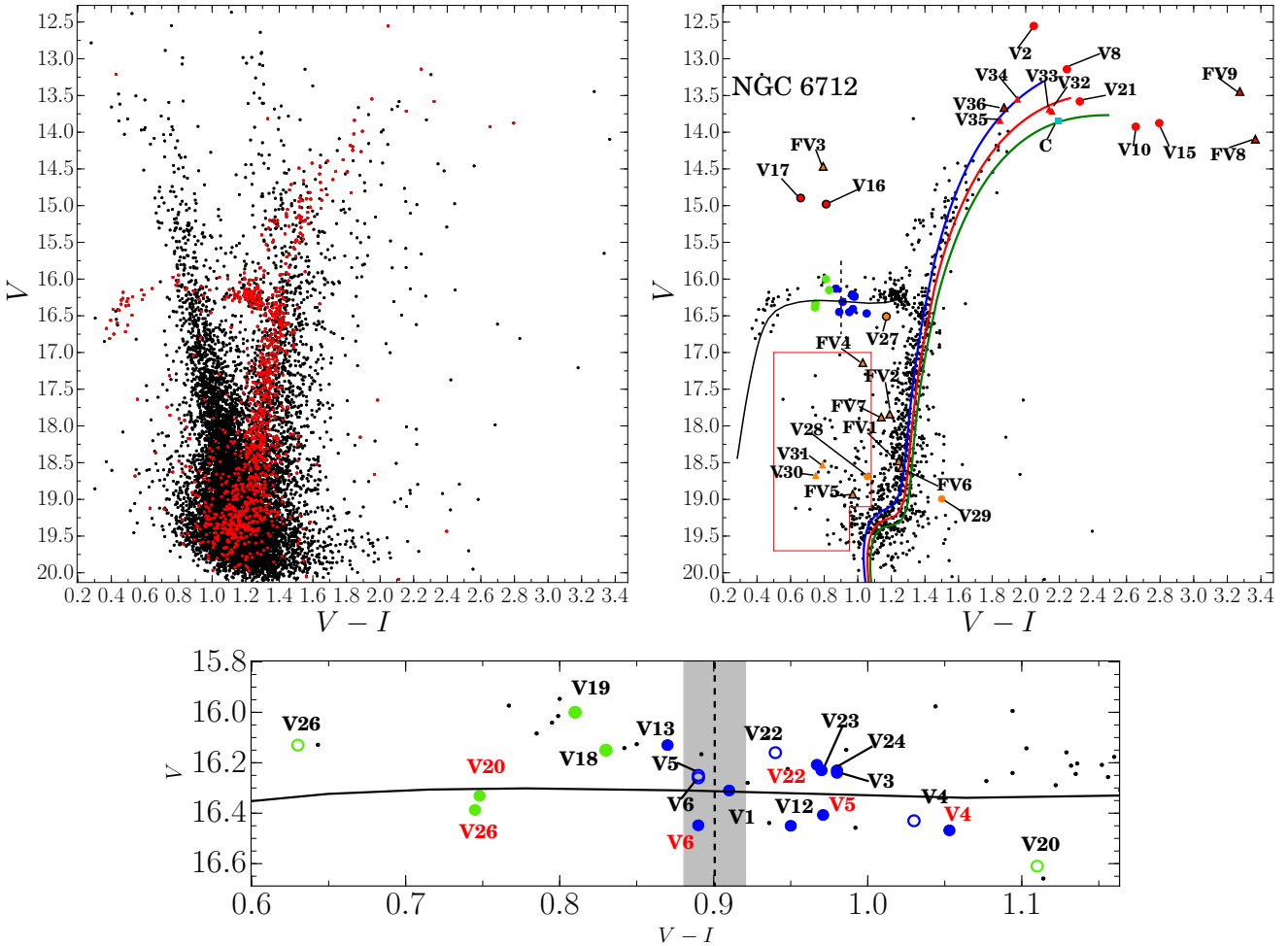


Figure 10. Colour-Magnitude Diagrams of NGC 6712 in VI filters. The left panel shows the CMD with all the measured stars in our FoV (black dots) and the likely star members (red dots). The right panel shows the likely star members once the CMD has been cleaned of field stars following the method described in § 3. The right panel also shows the known and newly discovered variables. We possess the light curves of 1100 stars (members and non-members). The blue circles correspond to RRab stars, the green circles to RRc stars, the red circles to long-period stars and the orange circles to EW stars. Triangular markers are newly discovered stars. Markers with a black rim represent non-member variable stars. The cyan square represents a candidate variable star. The isochrones in the right panel are 12 Gyr interpolations for $[\text{Fe}/\text{H}]$ values -1.25 (blue), -1.0 (red) and -0.86 (green). See § 8 for a discussion on the average metallicity. All three isochrones were created using $Y=0.25$ and $[\alpha/\text{Fe}]=+0.4$, from the model grid of VandenBerg et al. (2014). The isochrones and the ZAHB (black line) have been shifted to a distance of 8.1 kpc and reddened by $E(B-V)=0.35$. The red box delimits the region where blue straggler stars are found (see 8.2 for details). The lower panel shows an expansion of the HB for clarity purposes. The open blue and green circles correspond to the original position of the RR Lyrae before their magnitude and colour were corrected due a contaminating neighbouring star. The red tags accompany the new position after the correction. The dashed vertical line represents the FORE of the instability strip as estimated by Arellano Ferro et al. (2016) with its uncertainty in grey.

The cluster, in its current stage within its tidal radius, keeps itself rather compact. This allows it to better withstand its gravitational interaction with the Galactic bulge and the Galactic plane now than in the past, when it was much more massive and extended. It is possible that its compactness allows the cluster to preserve its tidal identity for many more encounters to come.

10 SUMMARY AND CONCLUSIONS

In this paper we have performed high-precision VI CCD photometry of 11294 stars in the FoV of globular cluster NGC 6712. Our main goal was to obtain physical parameters of the RR Lyrae star population via Fourier decomposition of their light curves. This method yielded metallicities of $[\text{Fe}/\text{H}]_{\text{ZW}} = -1.25 \pm 0.02$ and

$[\text{Fe}/\text{H}]_{\text{ZW}} = -1.10 \pm 0.16$ for the RRab and RRc stars respectively with a weighted mean of $[\text{Fe}/\text{H}]_{\text{ZW}} = -1.23 \pm 0.02$ using the calibrations by Jurcsik & Kovács (1996) and Morgan et al. (2007). For comparison we estimated the metallicities using the calibration derived by Nemec et al. (2013) and Nemec et al. (2011) which are given in the HDS scale $[\text{Fe}/\text{H}]_{\text{UVES}}^{\text{N13}} = -0.82 \pm 0.06$ for the RRab stars and $[\text{Fe}/\text{H}]_{\text{UVES}}^{\text{N13}} = -0.96 \pm 0.19$ for RRc stars yielding a weighted mean of $[\text{Fe}/\text{H}]_{\text{UVES}}^{\text{N13}} = -0.85 \pm 0.05$. The above values are, within the uncertainties, in good agreement with the value reported by Harris (1996) of $[\text{Fe}/\text{H}] = -1.02$.

NGC 6712 is currently located inside the bulge of the Galaxy and therefore, it is highly contaminated by field stars. A proper motion analysis of 60,447 stars in our FoV was carried out in order to determine membership status and yielded 1529 likely members or

Table 10. Data of RR Lyrae stars (in bold face) in the field of NGC 6712, which show flux contamination from an adjacent star (within the PSF) from *Gaia*-DR2.

Variable	<i>Gaia</i> -DR2 ID	<i>G</i>	$G_{BP} - G_{RP}$	V_{Gaia}	I_{Gaia}	$V - I_{Gaia}$	V_{mix}	Δ_V	I_{mix}	Δ_I	Amp _V	Amp _I
V4	4203849122517862144	16.154	1.239	16.446	15.362	1.084	16.408	0.038	15.347	0.015	0.58	0.35
V4	4203849122443611648	20.053		20.070	20.032	0.038						
V5	4203848778920519168	15.911	1.005	16.110	15.242	0.869	15.954	0.157	15.166	0.076	1.34	0.81
V5	4203848778846478080	18.114		18.132	18.093	0.038						
V6	4203848985005261312	16.147		16.164	16.126	0.038	15.976	0.188	15.938	0.188	1.06	0.66
V6	4203848985005260672	17.954		17.972	17.934	0.038						
V20	4203849083790434304	16.042	0.999	16.240	15.377	0.863	16.069	0.171	15.293	0.083	0.48	0.26
V20	4203849088158325760	18.143		18.161	18.123	0.038						
V22	4203849874064518016	15.945	1.115	16.186	15.216	0.969	16.138	0.048	15.196	0.021	0.61	0.40
V22	4203849878432420352	19.528		19.545	19.507	0.038						
V26	4203849466042002944	15.980	0.861	16.132	15.392	0.740	15.874	0.257	15.249	0.142	0.15	0.10
V26	4203849466042002816	17.545		17.563	17.525	0.038						

2.5%, for which we possess the light curves of 1100. This allowed us to plot a remarkably clean CMD and to overlay three theoretical isochrones using the models of [VandenBerg et al. \(2014\)](#) and the metallicity found from the Fourier decomposition of the light curves of the RR Lyrae stars. We found that these isochrones are consistent with an age of 12 Gyrs. We also used a theoretical ZAHB with similar metallicity to the isochrones to fit the observed HB. The cleaning of the CMD also allowed us to decrease the estimated number of BSS members in NGC 6712 down to 61, since after the membership analysis many of them turned out to be field stars. The distance derived by the methods mentioned in § 7 yielded a value of $\langle d \rangle = 8.1 \pm 0.2$ kpc, if a colour excess $E(B - V) = 0.35$ is assumed. Evidences have been discussed that this value could be as large as 0.40, in which case the same methods yield a distance of 7.5 ± 0.2 kpc.

Based on the their light curve morphology, their position on the Bailey diagram and the period analyses of the stars V22, V23 and V27 we were able to classify properly V22 as a RRab star, to reclassify V23 as a RRab and V27 as a EW star. Furthermore, V22 and V23 are both on the right side of the FORE, where only RRab stars are expected to be found.

From the average of the periods of the RRab stars in the cluster ($\langle P \rangle = 0.58$), and the distribution of RRab and RRc star in the period-amplitude diagram, we confirm that NGC 6712 is a OoI-type cluster. We detected a mild Blazhko effect in the amplitude of V6. We additionally found nine new EW variables (V30 and V31 and FV1-FV7) and seven SR-type variables (V32-V36 and FV8-FV9). For five of these SR-type (V32, V36, FV8, FV9 and a candidate C), we were able to derive periods ranging between 12-31 days.

There are numerous evidences in the literature that NGC 6712 is a remnant of a much more massive cluster that has been tidally disrupted by its numerous encounters with the Galactic bulge. We were able, from the proper motion analysis, to find evidence that the present cluster is in fact a compact core that seems to retain its identity in spite of the gravitational interaction with the Galactic bulge and disc. The proper motion of some of the field variable stars are parallel to the galactic longitude and point towards the Galactic center, suggesting that they are field stars participating in the Galactic rotation, not necessarily being gravitationally stripped away. As of now, we do not have a method to properly differentiate star members that are being currently stripped away from the clus-

ter from the ones that belong to the field. It is possible that what we are seeing now is nothing more than the remaining core.

ACKNOWLEDGEMENTS

We are grateful to Dr. Raúl Michel Murillo for kindly providing the standard stars in the field of NGC 6712. We thank the staff of IAO, Hanle and CREST, Hosakote, that made these observations possible. The facilities at IAO and CREST are operated by the Indian Institute of Astrophysics, Bangalore. This project was partially supported by DGAPA-UNAM (Mexico) via grant IN106615-17. DD thanks CONACyT for the PhD scholarship. We have made extensive use of the SIMBAD and ADS services.

REFERENCES

- Allen C., 1990, *Revista Mexicana de Astronomía y Astrofísica*, **20**, 67
 Andreuzzi G., De Marchi G., Ferraro F. R., Paresce F., Pulone L., Buonoanno R., 2001, *A&A*, **372**, 851
 Arceo-Díaz S., Schröder K.-P., Zuber K., Jack D., 2015, *Rev. Mex. Astron. Astrofis.*, **51**, 151
 Arellano Ferro A., Giridhar S., Bramich D. M., 2010, *MNRAS*, **402**, 226
 Arellano Ferro A., Mancera Piña P. E., Bramich D. M., Giridhar S., Ahumada J. A., Kains N., Kuppuswamy K., 2015, *MNRAS*, **452**, 727
 Arellano Ferro A., Luna A., Bramich D. M., Giridhar S., Ahumada J. A., Muneer S., 2016, *Ap&SS*, **361**, 175
 Arellano Ferro A., Bustos Fierro I. H., Calderón J. H., Ahumada J. A., 2019, *Rev. Mex. Astron. Astrofis.*, **55**, 337
 Awadalla N. S., Hanna M. A., 2005, *Journal of Korean Astronomical Society*, **38**, 43
 Baumgardt H., Hilker M., Sollima A., Bellini A., 2019, *MNRAS*, **482**, 5138
 Bramich D. M., 2008, *MNRAS*, **386**, L77
 Bramich D. M., Freudling W., 2012, *MNRAS*, **424**, 1584
 Bramich D. M., Figueroa Jaimes R., Giridhar S., Arellano Ferro A., 2011, *MNRAS*, **413**, 1275
 Bramich D. M., et al., 2013, *MNRAS*, **428**, 2275
 Bramich D. M., Bachelet E., Alsubai K. A., Mislis D., Parley N., 2015, *A&A*, **577**, A108
 Burke Edward W. J., Rolland W. W., Boy W. R., 1970, *Journal of the Royal Astronomical Society of Canada*, **64**, 353
 Bustos Fierro I. H., Calderón J. H., 2019, *MNRAS*, **488**, 3024
 Cacciari C., Corwin T. M., Carney B. W., 2005, *AJ*, **129**, 267
 Carretta E., Bragaglia A., Gratton R., D’Orazi V., Lucatello S., 2009, *A&A*, **508**, 695

Catelan M., Pritzl B. J., Smith H. A., 2004, *ApJS*, **154**, 633

Chen X., Deng L., de Grijs R., Wang S., Feng Y., 2018, *ApJ*, **859**, 140

Clement C. M., et al., 2001, *AJ*, **122**, 2587

Cudworth K. M., 1988, *AJ*, **96**, 105

Dauphole B., Geffert M., Colin J., Ducourant C., Odenkirchen M., Tucholke H. J., 1996, *Astronomy and Astrophysics*, **313**, 119

Dworetzky M. M., 1983, *MNRAS*, **203**, 917

Ferraro F. R., Messineo M., Fusi Pecci F., de Palo M. A., Straniero O., Chieffi A., Limongi M., 1999a, *AJ*, **118**, 1738

Ferraro F. R., Paltrinieri B., Rood R. T., Dorman B., 1999b, *ApJ*, **522**, 983

Gaia Collaboration et al., 2018, *A&A*, **616**, A1

Guldenschuh K. A., et al., 2005, *PASP*, **117**, 721

Harris W. E., 1996, *AJ*, **112**, 1487

Harwood M., 1960, *Annalen van de Sterrewacht te Leiden*, **21**, 387

Homer L., Charles P. A., Naylor T., van Paradijs J., Auriere M., Koch-Miramond L., 1996, *MNRAS*, **282**, L37

Huang Y., Liu X. W., Yuan H. B., Xiang M. S., Chen B. Q., Zhang H. W., 2015, *MNRAS*, **454**, 2863

Janulis R., Smriglio F., 1992, *Baltic Astronomy*, **1**, 430

Jurcsik J., 1995, *Acta Astron.*, **45**, 653

Jurcsik J., 1998, *A&A*, **333**, 571

Jurcsik J., Kovács G., 1996, *A&A*, **312**, 111

Kovács G., Kanbur S. M., 1998, *MNRAS*, **295**, 834

Kovács G., Walker A. R., 2001, *A&A*, **374**, 264

Kunder A., et al., 2013, *AJ*, **146**, 119

Landolt A. U., 1983, *AJ*, **88**, 439

Lázaro C., Arévalo M. J., Almenara J. M., 2009, *New Astron.*, **14**, 528

Lee Y.-W., 1990, *ApJ*, **363**, 159

Lee M. G., Freedman W. L., Madore B. F., 1993, *ApJ*, **417**, 553

Morgan S. M., Wahl J. N., Wiecekhorst R. M., 2007, *MNRAS*, **374**, 1421

Nemec J. M., et al., 2011, *Monthly Notices of the Royal Astronomical Society*, **417**, 1022

Nemec J. M., Cohen J. G., Ripepi V., Deras A., Moskalik P., Sesar B., Chadid M., Bruntt H., 2013, *ApJ*, **773**, 181

Oosterhoff P. T., 1943, *Bulletin of the Astronomical Institutes of the Netherlands*, **9**, 399

Ortolani S., Momany Y., Barbay B., Bica E., Catelan M., 2000, *A&A*, **362**, 953

Paltrinieri B., Ferraro F. R., Paresce F., De Marchi G., 2001, *AJ*, **121**, 3114

Pietrukowicz P., Kaluzny J., 2004, *Acta Astron.*, **54**, 19

Pryor C., Meylan G., 1993, in Djorgovski S. G., Meylan G., eds, *Astronomical Society of the Pacific Conference Series Vol. 50, Structure and Dynamics of Globular Clusters*. p. 357

Ribeiro de Souza J., 2017, Master thesis, Universidade Federal do Rio Grande do Sul, Brazil

Rosino L., 1966, *ApJ*, **144**, 903

Salaris M., Cassisi S., 1997, *MNRAS*, **289**, 406

Salaris M., Chieffi A., Straniero O., 1993, *ApJ*, **414**, 580

Sandage A., Cacciari C., 1990, *ApJ*, **350**, 645

Sandage A., Smith L. L., Norton R. H., 1966, *ApJ*, **144**, 894

Sawyer H. B., 1953, *J. R. Astron. Soc. Canada*, **47**, 229

Schlafly E. F., Finkbeiner D. P., 2011, *ApJ*, **737**, 103

Schlegel D. J., Finkbeiner D. P., Davis M., 1998, *ApJ*, **500**, 525

Simon N. R., Clement C. M., 1993, *ApJ*, **410**, 526

Sloan G. C., et al., 2010, *ApJ*, **719**, 1274

Smolec R., 2005, *Acta Astronomica*, **55**, 59

Stetson P. B., 2000, *PASP*, **112**, 925

Sturch C., 1966, *ApJ*, **143**, 774

Tuairisg S. Ó., Butler R. F., Shearer A., Redfern R. M., Butler D., Penny A., 2003, *MNRAS*, **345**, 960

VandenBerg D. A., Bergbusch P. A., Ferguson J. W., Edvardsson B., 2014, *ApJ*, **794**, 72

Viaux N., Catelan M., Stetson P. B., Raffelt G. G., Redondo J., Valcarce A. A. R., Weiss A., 2013, *A&A*, **558**, A12

Yepez M. A., Arellano Ferro A., Schröder K. P., Muneer S., Giridhar S., Allen C., 2019, *New Astronomy*, **71**, 1

Zhang T., Ramakrishnan R., Livny M., 1996, *SIGMOD Rec.*, **25**, 103

Zinn R., West M. J., 1984, *ApJS*, **55**, 45

de Marchi G., Leibundgut B., Paresce F., Pulone L., 1999, *A&A*, **343**, L9

van Albada T. S., Baker N., 1971, *ApJ*, **169**, 311

APPENDIX A: FIELD VARIABLE AND PECULIAR STARS

A1 The case of V7

This variable was discovered by Sawyer (1953) and classified as a Mira-type star by Sloan et al. (2010), who were able to derive a pulsation period of 193.0 days. Our data span only 30 days but it displays a clear variation (see Fig. 8). These are evolved stars that during their evolution on the AGB can produce and expel dust into the interstellar medium, affecting their local reddening. In the case of V7, its location on the CMD is extremely shifted to the red probably due to its own dust shrouding. Hence, it is not labelled in Fig. 10 due to scale reasons. Its CMD coordinates are (4.701, 16.98). According to the membership analysis carried out in § 3, the star is a cluster member.

A2 The case of V14, V16 and V17

None of these three stars is a cluster member according to the analysis described in § 3, in agreement with the proper motion analysis performed by Cudworth (1988) for V17. The SR star V14 is not in the FoV of our images but in terms of variability, V14 is a clear variable (Rosino 1966). V16 and V17 were flagged as variables by Harwood (1960), but Rosino (1966) and Sandage et al. (1966) did not detect any variability. Unfortunately the light curves of V16 and V17 were not published by previous authors. The light curves in our data are shown in Fig. 8, where subtle but clear signs of long-term variations can be seen.

A3 The case of V22

Cudworth (1988) noted that this star showed low amplitude variations and that given its position on the CMD, it could presumably be catalogued as a RR Lyrae. In the Catalogue of Variable Stars in Globular Clusters (CVSGC) Clement et al. (2001) the star is designated as RR type and its period is not provided. V22 is also located near the locus where RRab stars in OoI-type clusters are expected to be found in the Period-Amplitude diagram (Fig. 7). The shape of the light curve (see Fig. 6), its amplitude, position on the Horizontal Branch (HB) (Fig. 10) and period ($P = 0.654789d$), clearly indicate its RRab nature.

A4 The case of V23

This star, discovered by Tuairisg et al. (2003) (P1 in their paper), has been classified as RRc. Nevertheless, its reported period in the CVSGC of $P = 0.3896d$ does not phase the curve well. Moreover, using our 7 year time-base data, we found a period of $P = 0.642451d$ which is more consistent with a RRab star. Also, like V22, its position on the HB (Fig. 10) and on the Bailey diagram (Fig. 7) along with the shape of its light curve (Fig. 6) are all consistent with the star being a RRab.

A5 The case of V25

This is a low-mass X-ray binary discovered by Homer et al. (1996). According to these authors the optical counterpart shows variability and has a mean magnitude $V = 20.34 \pm 0.07$, i.e. too faint for our

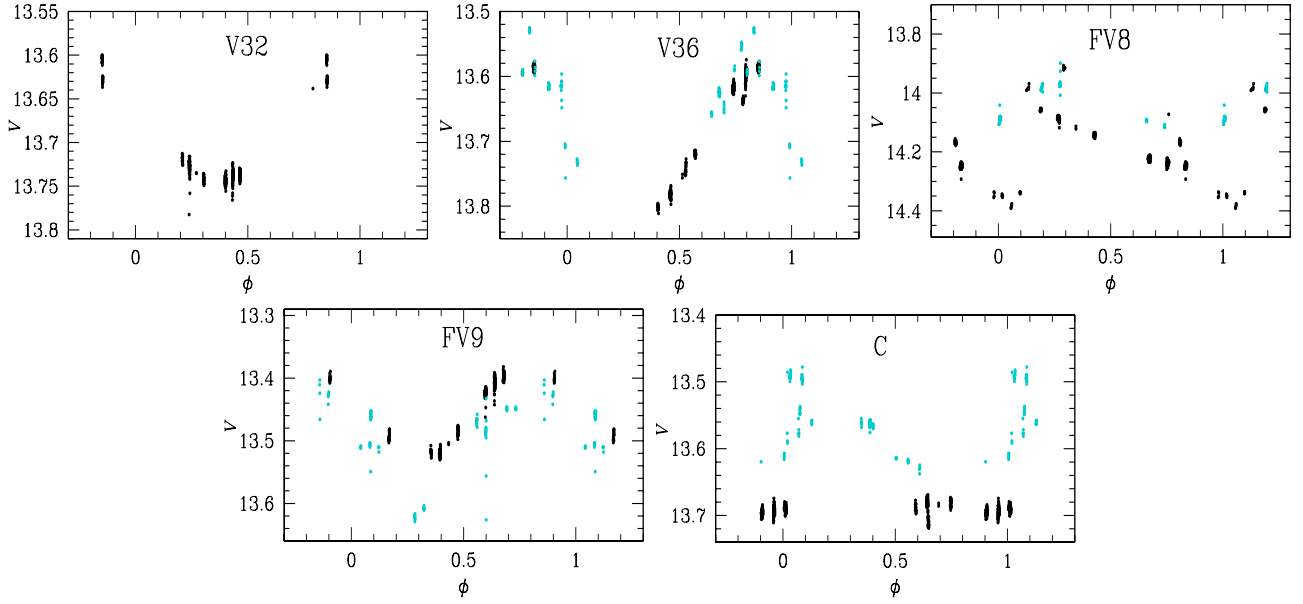


Figure A1. SR stars that could be phased with a single period, given in Tables 3 and 4.

CCD photometry. The nearest optical source in our images, to the coordinates listed by the CVSGC, is a $V \sim 16$ mag star which shows no variations.

A6 The case of V27

This star was discovered and classified as RRc by Pietrukowicz & Kaluzny (2004) (NGC6712_07 in their paper). These authors noted that the star showed an "unstable light curve with some cycle-to-cycle changes". We found that once it is phased with a period of $P = 0.425714d$ (which is approximately twice the reported value by Pietrukowicz & Kaluzny (2004)) the light curve of V27 (Fig. 6) shows alternating deep and shallow minima typical of EW stars. Hence, the star should be considered a short-period contact eclipsing binary.

A7 Semi-regular red variables

For five stars among the SR variables, a period that seems to phase all the available data was identified and are given in Tables 3 and 4. These stars and their phased light curves are shown in Fig. A1. Their amplitudes are of a few tenths of a magnitude and their periods range between 12 and 31 days. This suggests a classification as of the semiregular or SRs type.

This paper has been typeset from a \LaTeX file prepared by the author.